Branching ratios and *CP* asymmetries of $B \to K\eta^{(\prime)}$ decays in the perturbative QCD approach

Zhen-Jun Xiao,* Zhi-Qing Zhang, Xin Liu, and Li-Bo Guo+

Department of Physics and Institute of Theoretical Physics, Nanjing Normal University, Nanjing, Jiangsu 210097, People's Republic of China

(Received 28 September 2008; published 1 December 2008)

We calculate the branching ratios and *CP*-violating asymmetries of the four $B \to K\eta^{(\prime)}$ decays in the perturbative QCD (pQCD) factorization approach. Besides the full leading-order contributions, the partial next-to-leading-order (NLO) contributions from the QCD vertex corrections, the quark-loops, and the chromomagnetic penguins are also taken into account. The NLO pQCD predictions for the *CP*-averaged branching ratios are $\mathrm{Br}(B^+ \to K^+\eta) \approx 3.2 \times 10^{-6}$, $\mathrm{Br}(B^\pm \to K^\pm\eta') \approx 51.0 \times 10^{-6}$, $\mathrm{Br}(B^0 \to K^0\eta) \approx 2.1 \times 10^{-6}$, and $\mathrm{Br}(B^0 \to K^0\eta') \approx 50.3 \times 10^{-6}$. The NLO contributions can provide a 70% enhancement to the LO $\mathrm{Br}(B \to K\eta')$, but a 30% reduction to the LO $\mathrm{Br}(B \to K\eta)$, which play the key role in understanding the observed pattern of branching ratios. The NLO pQCD predictions for the *CP*-violating asymmetries, such as $\mathcal{A}_{CP}^{\mathrm{dir}}(K_S^0\eta') \sim 2.3\%$ and $\mathcal{A}_{CP}^{\mathrm{mix}}(K_S^0\eta') \sim 63\%$, agree very well with currently available data. This means that the deviation $\Delta S = \mathcal{A}_{CP}^{\mathrm{mix}}(K_S^0\eta') - \sin 2\beta$ in pQCD approach is also very small.

DOI: 10.1103/PhysRevD.78.114001 PACS numbers: 13.25.Hw, 12.38.Bx, 14.40.Nd

I. INTRODUCTION

The $B \to K\eta^{(\prime)}$ decays are very interesting two-body charmless hadronic B meson decays. In 1997, the CLEO collaboration first reported unexpectedly large branching ratios for $B \to K\eta'$ decays [1]. Eleven years later, three of the four $B \to K\eta^{(\prime)}$ decays have been measured with high precision. The world averages as given by HFAG [2] are the following (in units of 10^{-6}):

$$\begin{aligned} \mathrm{Br}(B^\pm \to K^\pm\eta) &= 2.7 \pm 0.3, \\ \mathrm{Br}(B^\pm \to K^\pm\eta') &= 70.2 \pm 2.5, \\ \mathrm{Br}(B^0 \to K^0\eta) &< 1.9, \\ \mathrm{Br}(B^0 \to K^0\eta') &= 64.9 \pm 3.1. \end{aligned} \tag{1}$$

From the above data one can see that: (a) the measured $\mathrm{Br}(B \to K\eta')$ are much larger than the early standard model (SM) expectations, i.e., the so-called $k\eta'$-puzzle; and (b) the large disparity between the branching ratios for $B \to K\eta'$ and $B \to K\eta$ decays: $\mathrm{Br}(B \to K\eta') \gg \mathrm{Br}(B \to K\eta)$.

Besides the branching ratios, the *CP*-violating asymmetries for $B^\pm \to K^\pm\eta^{(\prime)}$ and $B^0 \to K^0\eta^{(\prime)}$ decays have been measured very recently [2,3]:

$$\begin{aligned} \mathcal{A}_{CP}^{\mathrm{dir}}(B^\pm \to K^\pm\eta) &= -0.27 \pm 0.09, \\ \mathcal{A}_{CP}^{\mathrm{dir}}(B^\pm \to K^\pm\eta') &= 0.016 \pm 0.019, \end{aligned} \tag{2}$$

$$\begin{aligned} \mathcal{A}_{CP}^{\mathrm{dir}}(B^0 \to K^0\eta') &= 0.09 \pm 0.06, \\ \mathcal{A}_{CP}^{\mathrm{mix}}(B^0 \to K^0\eta') &= 0.61 \pm 0.07. \end{aligned} \tag{3}$$

It may be noted that the average of the measured $\mathcal{A}_{CP}^{\mathrm{mix}}(B^0 \to K^0\eta')$ is now more than 8σ away from zero, so that *CP* violation in this decay is well established; while $\mathcal{A}_{CP}^{\mathrm{dir}}(B^0 \to K^0\eta')$ is not in conflict with zero as expected in the SM. The data for $\mathcal{A}_{CP}^{\mathrm{dir}}(B^\pm \to K^\pm\eta^{(\prime)})$ have less precision, but are consistent with general expectations.

The measurements of time-dependent *CP* asymmetries in B^0 meson decays, such as $B^0 \to J/\Psi K^0$ via $b \to c\bar{c}s$ "tree" transition and $B^0 \to K^0\eta'$ via $b \to sq\bar{q}$ penguin transition, have provided crucial tests of the mechanism of *CP* violation in the SM. Within the SM the mixing-induced *CP*-violating asymmetry $\mathcal{A}_{CP}^{\mathrm{mix}}(B^0 \to K^0\eta') = -\eta_f S_f$ should be comparable with $\sin 2\beta = 0.685$ obtained from the tree-dominated $B^0 \to J/\Psi K^0$ decay; this point has been confirmed by the data in Eq. (3).

In the SM the decay $B \to K\eta^{(\prime)}$ is believed to proceed dominantly through gluonic penguin processes [4,5] and has been evaluated by employing various methods [6–16]. Although great progress has been made during the past decade, the predictions for $\mathrm{Br}(B \to K\eta')$ from both the QCD factorization (QCDF) approach [14,17] and the perturbative QCD (pQCD) approach [16,18] in the Feldmann-Kroll-Stech (FKS) mixing scheme of $\eta - \eta'$ system [19,20] are smaller than the data.

For the pattern of branching ratios in Eq. (1), many possible solutions have been proposed. These include, for example,

(a) Conventional $b \to sq\bar{q}$ with constructive (destructive) interference between the $u\bar{u}$, $d\bar{d}$ and $s\bar{s}$ components of η' (η) [4];
(b) Large intrinsic charm content of η' through the chain $b \to sc\bar{c} \to s\eta'$ [7] or through $b \to sc\bar{c} \to sg^*g^* \to s(\eta, \eta')$ due to the QCD anomaly [8];
(c) The spectator hard-scattering mechanism through the anomalous coupling of $gg \to \eta'$ [9–11];

*xiaozhenjun@njnu.edu.cn
+guolibo@njnu.edu.cn

(d) A significant flavor-singlet contribution [10,14];
(e) A strong penguin $b \to sg$ enhanced by new physics [12,13].

But the data of branching ratio in Eq. (1) are still not completely understood. For the CP violation of $B \to K\eta^{(\prime)}$ decays, the theoretical studies is still under way.

In Ref. [16], the authors calculated the branching ratios of $B \to K\eta^{(\prime)}$ decays by employing the pQCD approach at leading order. They considered the large corrections from $SU(3)$ flavor symmetry breaking as well as the possible gluonic component of the η' meson, but their prediction for $\mathrm{Br}(B^0 \to K^0\eta')$ ($\mathrm{Br}(B^0 \to K^0\eta)$) is much smaller (larger) than the measured value.

A sizable gluonic content in the η' meson may provide a large enhancement to the decay rate of $B \to K\eta'$. In Ref. [21], the authors examined the possible gluonic contribution to the $B \to \eta'$ transition form factor and found that such a contribution is constructive with those from the quark-content of η', but numerically very small and can be neglected safely. This point has also been confirmed by the QCD sum-rule analysis [22].

In the quark-flavor mixing scheme, the physical η and η' meson are linear combinations of flavor state $\eta_q = (u\bar{u} + d\bar{d})/\sqrt{2}$ and $\eta_s = s\bar{s}$ with the "mass" of m_{qq} and m_{ss} respectively. In Ref. [23], the effect of a large chiral scale $m_0^q = m_{qq}^2/(2m_q)$ with $q = (u, d)$ for the meson η_q has been evaluated although we do not know which mechanism is responsible to achieve a large value of m_{qq}. When one uses $m_{qq} = 0.22$ GeV [23] instead of its generally accepted value of $m_{qq} = 0.11$ GeV, a larger $B \to K\eta_q$ decay amplitude can be obtained. Consequently, the LO pQCD predictions for $\mathrm{Br}(B \to K\eta')$ become consistent with the data.

In Ref. [24], the authors examined the possible way to increase the value of m_{qq}. They found that a few-percent violation of the Okubo-Zweig-Iizuka (OZI) rule can enhance m_{qq} a few times, which then leads to the consistency of the LO predictions with the data for $B \to K\eta^{(\prime)}$ decays.

Besides the possible mechanisms mentioned above, we here consider a new and natural solution: the effects of the next-to-leading-order (NLO) contributions in the pQCD approach. As shown in Ref. [25], the NLO contributions to $B \to K\pi$ decays can play the key rule to explain the so-called "$K\pi$"-puzzle. We expect here that the NLO contributions could help us to resolve the "$K\eta'$"-puzzle.

For the CP asymmetries of $B^0 \to K^0\eta'$, the deviation $\Delta S_f = -\eta_f S_f - \sin 2\beta$ has been estimated, for example, in the QCDF approach [15,26] and the soft collinear effective theory [27]. The resultant bound is $|\Delta S_f| \lesssim 0.05$. Since the source of the CP violation in the pQCD approach is very different from those in the QCDF/SCET approach, we here try to calculate the CP asymmetries of $B \to K\eta^{(\prime)}$ decays by employing the pQCD approach at LO and NLO level, to check if we can accommodate the data of CP asymmetries.

In this paper we will calculate the next-to-leading-order contributions to the branching ratios and CP-violating asymmetries of the four $B \to K\eta^{(\prime)}$ decays. We first calculate the decay amplitudes of the $B \to K\eta^{(\prime)}$ decays by employing the pQCD factorization approach at the leading order, as have been done in previous studies for other two-body charmless B meson decays [28–31]. And then we evaluate the NLO contributions to these decays.

The NLO contributions considered here include: QCD vertex corrections, the quark-loops and the chromomagnetic penguins. We expect that they are the major part of the full NLO contributions in the pQCD approach [25]. Of course, remaining NLO contributions in the pQCD approach, such as those from factorizable emission diagrams, hard-spectator and annihilation diagrams, should be calculated as soon as possible.

This paper is organized as follows. In Sec. II, we give a brief review about the pQCD factorization approach. In Sec. III, we calculate analytically the relevant Feynman diagrams and present the various decay amplitudes for the studied decay modes in leading order. In Sec. IV, the NLO contributions from the vertex corrections, the quark loops and the chromomagnetic penguin amplitudes are evaluated. We calculate and show the pQCD predictions for the branching ratios and CP-violating asymmetries of $B \to K\eta^{(\prime)}$ decays in Sec. V. The summary and some discussions are included in the final section.

II. THEORETICAL FRAMEWORK

A. Theoretical framework

In the pQCD approach, the decay amplitude is separated into soft (Φ_{M_i}), hard ($H(k_i, t)$), and harder ($C(M_W)$) dynamics characterized by different energy scales (Λ_{QCD}, t, m_b, M_W) [18]. The decay amplitude $\mathcal{A}(B \to M_2M_3)$ can be written conceptually as the convolution,

$$\mathcal{A}(B \to M_2M_3) \sim \int d^4k_1 d^4k_2 d^4k_3 \mathrm{Tr}[C(t)\Phi_B(k_1) \times \Phi_{M_2}(k_2)\Phi_{M_3}(k_3)H(k_1, k_2, k_3, t)], \quad (4)$$

where k_i's are momenta of light quarks included in each meson, and Tr denotes the trace over Dirac and color indices. $C(t)$ is the Wilson coefficient evaluated at scale t. In the above convolution, the Wilson coefficient $C(t)$ includes the harder dynamics at scale higher than M_B and describes the evolution of local 4-Fermi operators from m_W (the W boson mass) down to $t \sim \mathcal{O}(\sqrt{\bar{\Lambda}M_B})$ scale, where $\bar{\Lambda} \equiv M_B - m_b$. The function $H(k_1, k_2, k_3, t)$ describes the four-quark operator and the spectator quark connected by a hard gluon whose q^2 is in the order of $\bar{\Lambda}M_B$, and includes the $\mathcal{O}(\sqrt{\bar{\Lambda}M_B})$ hard dynamics. Therefore, this hard kernel H can be perturbatively calculated. The function Φ_{M_i} is the wave function which describes hadronization of the quark

and antiquark in the meson M_i. While the hard kernel H depends on the processes considered, the wave function Φ_{M_i} is independent of the specific processes. Using the wave functions determined from other well-measured processes, one can make quantitative predictions here.

Since the b quark inside the B meson is rather heavy, we consider the B meson at rest for simplicity. It is then convenient to use light-cone coordinate $(p^+, p^-, \mathbf{p}_T)$ to describe the meson's momenta: $p^\pm = \frac{1}{\sqrt{2}}(p^0 \pm p^3)$ and $\mathbf{p}_T = (p^1, p^2)$. Using the light-cone coordinates the B meson momentum P_B and the two final state meson's momenta P_2 and P_3 (for M_2 and M_3 respectively) can be written as

$$P_B = \frac{M_B}{\sqrt{2}}(1, 1, \mathbf{0}_T), \qquad P_2 = \frac{M_B}{\sqrt{2}}(1 - r_3^2, r_2^2, \mathbf{0}_T), \qquad P_3 = \frac{M_B}{\sqrt{2}}(r_3^2, 1 - r_2^2, \mathbf{0}_T), \tag{5}$$

where $r_i = m_i/M_B$. m_2 and m_3 are the mass of the two final state mesons. For the case of $B \to PP$ decays, r_2 and r_3 are small and could be neglected safely.

Putting the antiquark momenta in the B, M_2 and M_3 meson as k_1, k_2, and k_3, respectively, we can choose

$$k_1 = (x_1 P_1^+, 0, \mathbf{k}_{1T}), \qquad k_2 = (x_2 P_2^+, 0, \mathbf{k}_{2T}), \qquad k_3 = (0, x_3 P_3^-, \mathbf{k}_{3T}). \tag{6}$$

Then, the integration over k_1^-, k_2^-, and k_3^+ in Eq. (4) will lead to

$$\mathcal{A}(B \to PV) \sim \int dx_1 dx_2 dx_3 b_1 db_1 b_2 db_2 b_3 db_3 \cdot \mathrm{Tr}[C(t)\Phi_B(x_1, b_1)\Phi_{M_2}(x_2, b_2)\Phi_{M_3}(x_3, b_3) \times H(x_i, b_i, t) S_t(x_i) e^{-S(t)}], \tag{7}$$

where b_i is the conjugate space coordinate of k_{iT}. The large logarithms ($\ln m_W/t$) coming from QCD radiative corrections to four-quark operators are included in the Wilson coefficients $C(t)$. The large double logarithms ($\ln^2 x_i$) on the longitudinal direction are summed by the threshold resummation, and they lead to $S_t(x_i)$ which smears the end-point singularities on x_i. The last term, $e^{-S(t)}$, is the Sudakov form factor which suppresses the soft dynamics effectively [18].

B. Effective Hamiltonian and Wilson coefficients

For the studied $B \to K\eta^{(\prime)}$ decays, the weak effective Hamiltonian H_{eff} for $b \to s$ transition can be written as [32]

$$\mathcal{H}_{\mathrm{eff}} = \frac{G_F}{\sqrt{2}} \sum_{q=u,c} V_{qb} V_{qs}^* \Big\{ [C_1(\mu) O_1^q(\mu) + C_2(\mu) O_2^q(\mu)] + \sum_{i=3}^{10} C_i(\mu) O_i(\mu) \Big\}, \tag{8}$$

where $G_F = 1.16639 \times 10^{-5}\ \mathrm{GeV}^{-2}$ is the Fermi constant, and V_{ij} is the Cabibbo-Kobayashi-Maskawa (CKM) matrix element, $C_i(\mu)$ are the Wilson coefficients evaluated at the renormalization scale μ, and $O_i(\mu)$ are the four-fermion operators. For the case of $b \to d$ transition, one simply makes a replacement of s by d in Eq. (8) and in the expressions of $O_i(\mu)$ operators, which can be found easily, for example, in Refs.[30–32].

In PQCD approach, the energy scale "t" is chosen as the largest energy scale in the hard kernel $H(x_i, b_i, t)$ of a given Feynman diagram, in order to suppress the higher-order corrections and improve the reliability of the perturbative calculation. Here, the scale "t" may be larger or smaller than the m_b scale. In the range of $t < m_b$ or $t \geq m_b$, the number of active quarks is $N_f = 4$ or $N_f = 5$, respectively. For the Wilson coefficients $C_i(\mu)$ and their renormalization group (RG) running, they are known at NLO level currently [32]. The explicit expressions of the LO and NLO $C_i(m_W)$ can be found easily, for example, in Refs. [29,32].

When the pQCD approach at leading-order is employed, the leading-order Wilson coefficients $C_i(m_W)$, the leading-order RG evolution matrix $U(t, m)^{(0)}$ from the high scale m down to $t < m$ (for details see Eq. (3.94) in Ref. [32]), and the leading-order $\alpha_s(t)$ are used:

$$\alpha_s(t) = \frac{4\pi}{\beta_0 \ln[t^2/\Lambda_{\mathrm{QCD}}^2]}, \tag{9}$$

where $\beta_0 = (33 - 2N_f)/3$, $\Lambda_{\mathrm{QCD}}^{(5)} = 0.225$ GeV, and $\Lambda_{\mathrm{QCD}}^{(4)} = 0.287$ GeV.

When the NLO contributions are taken into account, however, the NLO Wilson coefficients $C_i(m_W)$, the NLO RG evolution matrix $U(t, m, \alpha)$ (for details see Eq. (7.22) in Ref. [32]), and the $\alpha_s(t)$ at two-loop level are used:

$$\alpha_s(t) = \frac{4\pi}{\beta_0 \ln[t^2/\Lambda_{\mathrm{QCD}}^2]} \cdot \left\{ 1 - \frac{\beta_1}{\beta_0^2} \cdot \frac{\ln[\ln[t^2/\Lambda_{\mathrm{QCD}}^2]]}{\ln[t^2/\Lambda_{\mathrm{QCD}}^2]} \right\}, \tag{10}$$

where $\beta_0 = (33 - 2N_f)/3$, $\beta_1 = (306 - 38N_f)/3$, $\Lambda_{\mathrm{QCD}}^{(5)} = 0.225$ GeV, and $\Lambda_{\mathrm{QCD}}^{(4)} = 0.326$ GeV.

From the general knowledge, the hard scale t must be much larger than $\Lambda_{\mathrm{QCD}} \approx 0.2$ GeV in order to guarantee the reliability of perturbative calculations. In previous calculations based on the pQCD approach $\mu_0 = 0.5$ GeV is chosen as the lower cutoff of the scale t. In our opinion, it is indeed too low, because it may be conceptually incorrect to evaluate the Wilson coefficients at scales down to 0.5 GeV [33]. The explicit numerical checks as done in

Ref. [34] also show that (a) the Wilson coefficient $C_1(0.5)$ is close to -1 and clearly too large in size!; (b) the values of the Wilson coefficients $C_{3,4,5,6}(\mu)$ at $\mu = 0.5$ GeV are about 4 to 7 times larger than those at $\mu = 1.0$ GeV; and (c) the μ_0-dependence of all Wilson coefficients becomes relatively weak for $\mu_0 \geq 1.0$ GeV. We therefore believe that it is reasonable to choose $\mu_0 = 1.0$ GeV as the lower cutoff of the hard scale t, which is also close to the hard-collinear scale $\sqrt{\bar{\Lambda} m_B} \sim 1.3$ GeV in SCET. In the numerical integrations we will fix the values $C_i(t)$ at $C_i(1.0)$ whenever the scale t runs below the scale $\mu_0 = 1.0$ GeV [34,35].

C. Wave functions

Since the b-quark is much heavier than the up or down quark, the B meson is treated as a very good heavy-light system. Although there are in general two Lorentz structures in the B meson distribution amplitudes, they obey to the following normalization conditions:

$$\int \frac{d^4k_1}{(2\pi)^4}\phi_B(\mathbf{k_1}) = \frac{f_B}{2\sqrt{2N_c}}, \qquad \int \frac{d^4k_1}{(2\pi)^4}\bar{\phi}_B(\mathbf{k_1}) = 0. \tag{11}$$

However, it can be argued that the contribution of $\bar{\phi}_B$ is numerically small [36], thus its contribution can be numerically neglected. In this approximation, we only consider the contribution of Lorentz structure

$$\Phi_B = \frac{1}{\sqrt{2N_c}}(\not{P}_B + m_B)\gamma_5\phi_B(\mathbf{k_1}), \tag{12}$$

with

$$\phi_B(x,b) = N_B x^2(1-x)^2 \exp\left[-\frac{M_B^2 x^2}{2\omega_b^2} - \frac{1}{2}(\omega_b b)^2\right], \tag{13}$$

where ω_b is a free parameter and we take $\omega_b = 0.4 \pm 0.04$ GeV in numerical calculations, and $N_B = 101.445$ is the normalization factor for $\omega_b = 0.4$.

The Kaon mesons are treated as a light-light system. The wave function of K meson is defined as [37]

$$\Phi_K(P,x,\zeta) \equiv \frac{1}{\sqrt{2N_C}}\gamma_5[\not{P}\phi_K^A(x) + m_0^K\phi_K^P(x) + \zeta m_0^K(\not{v}\not{n} - v\cdot n)\phi_K^T(x)], \tag{14}$$

where P and x are the momentum and the momentum fraction of K, respectively. The parameter ζ is either $+1$ or -1 depending on the assignment of the momentum fraction x.

For the $\eta^{(\prime)}$ meson, the wave function for η_q components of η' meson are given as

$$\Phi_{\eta_q}(P,x,\zeta) \equiv \frac{1}{\sqrt{2N_C}}\gamma_5[\not{P}\phi_{\eta_q}^A(x) + m_0^q\phi_{\eta_q}^P(x) + \zeta m_0^q(\not{v}\not{n} - v\cdot n)\phi_{\eta_q}^T(x)], \tag{15}$$

where P and x are the momentum and the momentum fraction of η_q, respectively. We assumed here that the wave function of η_q is the same as the π wave function. The parameter ζ is either $+1$ or -1 depending on the assignment of the momentum fraction x. The $\eta_s = s\bar{s}$ component of the wave function can be defined in the same way.

The expressions of the relevant distribution amplitudes (DAs) of the K meson are the following [37]:

$$\phi_K^A(x) = \frac{f_K}{2\sqrt{2N_c}}6x(1-x)[1 + a_1^K C_1^{3/2}(t) + a_2^K C_2^{3/2}(t) + a_4^K C_4^{3/2}(t)], \tag{16}$$

$$\phi_K^P(x) = \frac{f_K}{2\sqrt{2N_c}}\left\{1 + \left(30\eta_3 - \frac{5}{2}\rho_K^2\right)C_2^{1/2}(t) - 3\left[\eta_3\omega_3 + \frac{9}{20}\rho_K^2(1+6a_2^K)\right]C_4^{1/2}(t)\right\}, \tag{17}$$

$$\phi_K^T(x) = -\frac{f_K}{2\sqrt{2N_c}}t\left[1 + 6\left(5\eta_3 - \frac{1}{2}\eta_3\omega_3 - \frac{7}{20}\rho_K^2 - \frac{3}{5}\rho_K^2 a_2^K\right)(1 - 10x + 10x^2)\right], \tag{18}$$

with the mass ratio $\rho_K = m_K/m_{0K}$. The Gegenbauer moments can be given as [37]:

$$a_1^K = 0.2, \qquad a_2^K = 0.25, \qquad a_4^K = -0.015. \tag{19}$$

The values of other parameters are $\eta_3 = 0.015$ and $\omega = -3.0$. At last the Gegenbauer polynomials $C_n^\nu(t)$ are given as

$$\begin{aligned} C_2^{1/2}(t) &= \frac{1}{2}(3t^2 - 1), \\ C_4^{1/2}(t) &= \frac{1}{8}(3 - 30t^2 + 35t^4), \\ C_1^{3/2}(t) &= 3t, \qquad C_2^{3/2}(t) = \frac{3}{2}(5t^2 - 1), \\ C_4^{3/2}(t) &= \frac{15}{8}(1 - 14t^2 + 21t^4), \end{aligned} \tag{20}$$

with $t = 2x - 1$.

In the quark-flavor mixing scheme, the physical states η and η' are related to the flavor states $\eta_q = (u\bar{u} + d\bar{d})/\sqrt{2}$ and $\eta_s = s\bar{s}$ through a single mixing angle ϕ,

$$\begin{pmatrix}\eta \\ \eta'\end{pmatrix} = \begin{pmatrix}\cos\phi & -\sin\phi \\ \sin\phi & \cos\phi\end{pmatrix}\begin{pmatrix}\eta_q \\ \eta_s\end{pmatrix} = \begin{pmatrix}F_1(\phi)(u\bar{u} + d\bar{d}) + F_2(\phi)s\bar{s} \\ F_1'(\phi)(u\bar{u} + d\bar{d}) + F_2'(\phi)s\bar{s}\end{pmatrix} \tag{21}$$

with

$$F_1(\phi)=\frac{\cos\phi}{\sqrt{2}}, \qquad F_2(\phi)=-\sin\phi,$$
$$F_1'(\phi)=\frac{\sin\phi}{\sqrt{2}}, \qquad F_2'(\phi)=\cos\phi. \tag{22}$$

The relation between the decay constants $(f_\eta^q, f_\eta^s, f_{\eta'}^q, f_{\eta'}^s)$ and $(f_q, f_s,)$ can be written as

$$\begin{pmatrix} f_\eta^q & f_\eta^s \\ f_{\eta'}^q & f_{\eta'}^s \end{pmatrix} = \begin{pmatrix} \cos\phi & -\sin\phi \\ \sin\phi & \cos\phi \end{pmatrix} \begin{pmatrix} f_q & 0 \\ 0 & f_s \end{pmatrix}. \tag{23}$$

The chiral enhancement m_0^q and m_0^s associated with the two-parton twist-3 η_q and η_s meson distribution amplitudes have been defined as [25]

$$m_0^q = \frac{m_{qq}^2}{2m_q} = \frac{1}{2m_q}\Big[m_\eta^2\cos^2\phi + m_{\eta'}^2\sin^2\phi - \frac{\sqrt{2}f_s}{f_q}(m_{\eta'}^2 - m_\eta^2)\cos\phi\sin\phi\Big], \tag{24}$$

$$m_0^s = \frac{m_{ss}^2}{2m_s} = \frac{1}{2m_s}\Big[m_{\eta'}^2\cos^2\phi + m_\eta^2\sin^2\phi - \frac{\sqrt{2}f_q}{f_s}(m_{\eta'}^2 - m_\eta^2)\cos\phi\sin\phi\Big], \tag{25}$$

by assuming the exact isospin symmetry $m_q = m_u = m_d$. The three input parameters f_q, f_s, and ϕ have been extracted from the data of the relevant exclusive processes [19]:

$$f_q = (1.07\pm 0.02)f_\pi, \qquad f_s = (1.34\pm 0.06)f_\pi, \qquad \phi = 39.3^\circ \pm 1.0^\circ. \tag{26}$$

The distribution amplitudes $\phi_{\eta_q}^{A,P,T}$ represent the axial-vector, pseudoscalar and tensor component of the wave function respectively [37]. They are given as

$$\phi_{\eta_q}^A(x) = \frac{f_q}{2\sqrt{2N_c}}6x(1-x)[1 + a_1^{\eta_q}C_1^{3/2}(2x-1) + a_2^{\eta_q}C_2^{3/2}(2x-1) + a_4^{\eta_q}C_4^{3/2}(2x-1)], \tag{27}$$

$$\phi_{\eta_q}^P(x) = \frac{f_q}{2\sqrt{2N_c}}\Big[1 + \Big(30\eta_3 - \frac{5}{2}\rho_{\eta_q}^2\Big)C_2^{1/2}(2x-1) - 3\Big\{\eta_3\omega_3 + \frac{9}{20}\rho_{\eta_q}^2(1+6a_2^{\eta_q})\Big\}C_4^{1/2}(2x-1)\Big], \tag{28}$$

$$\phi_{\eta_q}^T(x) = \frac{f_q}{2\sqrt{2N_c}}(1-2x)\Big[1 + 6\Big(5\eta_3 - \frac{1}{2}\eta_3\omega_3 - \frac{7}{20}\rho_{\eta_q}^2 - \frac{3}{5}\rho_{\eta_q}^2 a_2^{\eta_q}\Big)\cdot(1-10x+10x^2)\Big], \tag{29}$$

where $\rho_{\eta_q} = 2m_q/m_{qq}$, $a_1^{\eta_q} = a_1^\pi = 0$, $a_2^{\eta_q} = a_2^\pi = 0.44 \pm 0.22$, $a_4^{\eta_q} = a_4^\pi = 0.25$, and the Gegenbauer polynomials $C_n^\nu(t)$ have been given in Eq. (20). As to the wave function and the corresponding DAs of the $s\bar{s}$ components, we also use the same form as $q\bar{q}$ but with some parameters changed: $\rho_{\eta_s} = 2m_s/m_{ss}$, $a_i^{\eta_s} = a_i^{\eta_q}$ for $i = 1, 2, 4$.

The transverse momentum k_T is usually converted to the b parameter by Fourier transformation. The initial conditions of leading twist $\phi_i(x)$, $i = B, K, \eta, \eta'$, are of non-perturbative origin, satisfying the normalization

$$\int_0^1 \phi_i(x, b=0)dx = \frac{1}{2\sqrt{6}}f_i, \tag{30}$$

with f_i the meson decay constant.

III. DECAY AMPLITUDES AT LEADING ORDER

In the pQCD approach, the Feynman diagrams as shown in Fig. 1 may contribute to $B \to K\eta^{(\prime)}$ decays at leading order. As mentioned previously, $B^0 \to K^0\eta^{(\prime)}$ decays have been studied in Ref. [16] by employing the LO pQCD approach. In this section, we first calculate the LO decay amplitudes for four $B \to K\eta^{(\prime)}$ decays, but in a rather different way to treat the Feynman diagrams from that in Ref. [16].

At the leading order in the pQCD approach, there are three types of diagrams contributing to the $B \to K\eta^{(\prime)}$ decays, the factorizable emission diagrams, the hard-spectator diagrams, and the annihilation diagrams, as illustrated in Fig. 1. From the factorizable emission diagrams, the corresponding form factors can be extracted by perturbative calculation. First, we consider the $B \to K\eta$ decay modes, and then extend the calculation to $B \to K\eta'$ decays.

For the usual factorizable emission diagrams (Figs. 1(a) and 1(b)) with the $B \to K$ transition, i.e., it is the K meson pick up the spectator quark, the operators O_1, O_2, $O_{3,4}$, and $O_{9,10}$ are $(V-A)(V-A)$ currents, the sum of the individual amplitudes is given as

$$F_{eK} = \frac{8}{\sqrt{2}}\pi G_F C_F m_B^4 \int_0^1 dx_1 dx_2 \int_0^\infty b_1 db_1 b_2 db_2 \phi_B(x_1, b_1) \times \{[(1+x_2)\phi_K^A(\bar{x}_2) + (1-2x_2)r_K(\phi_K^P(\bar{x}_2) - \phi_K^T(\bar{x}_2))]\cdot E_e(t_a)h_e(x_1, x_2, b_1, b_2) + 2r_K\phi_K^P(\bar{x}_2)\cdot E_e(t_a')h_e(x_2, x_1, b_2, b_1)\}, \tag{31}$$

where $r_K = m_0^K/m_B$ with m_0^K is the chiral scale, $C_F = 4/3$

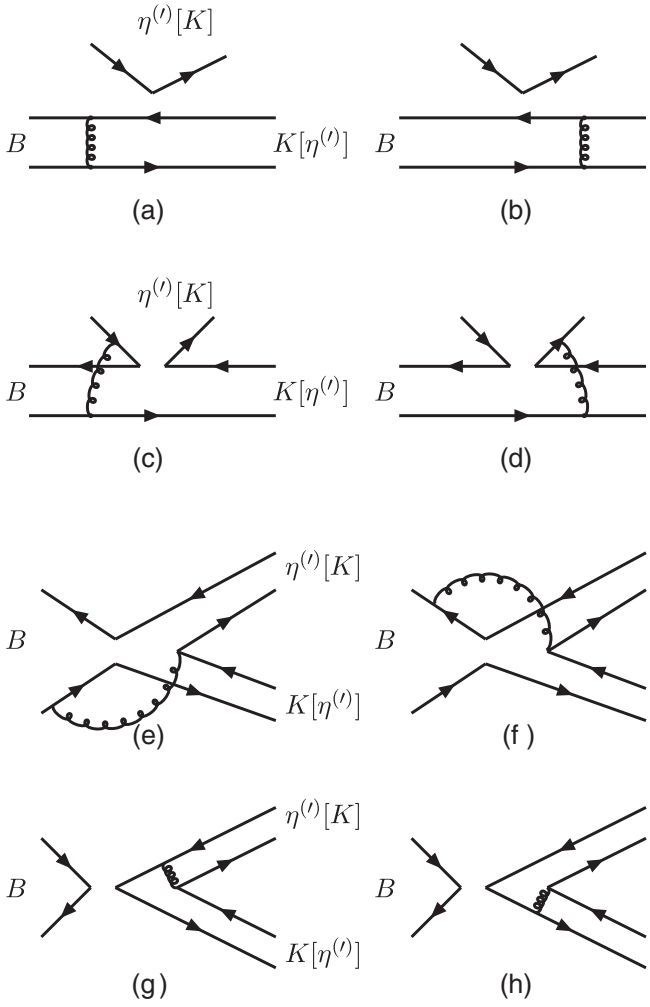

FIG. 1. Feynman diagrams which may contribute to the $B \to K\eta^{(\prime)}$ decays at leading order.

is a color factor, and $\bar{x}_2 = 1 - x_2$. The evolution function $E_e(t)$ and hard function h_e are displayed in the Appendix. In the above equation, we do not include the Wilson coefficients of the corresponding operators, which are process dependent. They will be shown later in the expressions of total decay amplitude.

Also for Figs. 1(a) and 1(b), the operators $O_{5,6}$ and $O_{7,8}$ have a structure of $(V - A)(V + A)$ currents. In some decay channels, some of these operators contribute to the decay amplitude in a factorizable way. Since only the axial-vector part of the $(V + A)$ current contributes to the pseudoscaler meson production, $\langle K|V - A|B\rangle \times \langle \eta^{(\prime)}|V + A|0\rangle = -\langle K|V - A|B\rangle\langle \eta^{(\prime)}|V - A|0\rangle$, that is

$$F_{eK}^{P1} = -F_{eK}. \tag{32}$$

In some other cases, we need to do Fierz transformation for those operators to get the right color structure for factorization to work. In this case, we get $(S - P)(S + P)$ operators from $(V - A)(V + A)$ ones. For these $(S - P)(S + P)$ operators, the corresponding decay amplitude is

$$\begin{aligned} F_{eK}^{P2} = {} & \frac{16}{\sqrt{2}}\pi G_F C_F m_B^4 \int_0^1 dx_1 dx_2 \int_0^\infty b_1 db_1 b_2 db_2 \phi_B(x_1) \\ & \times \{r_\eta[\phi_K^A(\bar{x}_2) + r_K((2 + x_2)\phi_K^P(\bar{x}_2) + x_2\phi_K^T(\bar{x}_2))] \\ & \cdot E_e(t_a) h_e(x_1, x_2, b_1, b_2) + 2r_K r_\eta \phi_K^P(\bar{x}_2) \\ & \cdot E_e(t_a') h_e(x_2, x_1, b_2, b_1)\}, \end{aligned} \tag{33}$$

where $r_\eta = m_0^q/m_B$, and $m_0^q = m_0^{\eta_q}$ is the chiral scale defined in Eq. (24).

For the nonfactorizable diagrams (Figs. 1(c) and 1(d)), all three meson wave functions are involved. The integration of b_2 can be performed using the δ function $\delta(b_3 - b_2)$, leaving only integration of b_1 and b_3. For the $(V - A)(V - A)$ operators, the result is

$$\begin{aligned} M_{eK} = {} & \frac{16}{\sqrt{3}}\pi G_F C_F m_B^4 \int_0^1 dx_1 dx_2 dx_3 \int_0^\infty b_1 db_1 b_3 db_3 \\ & \times \phi_B(x_1, b_1)\phi_\eta^A(\bar{x}_3)\{[-r_K x_2(\phi_K^P(\bar{x}_2) + \phi_K^T(\bar{x}_2)) \\ & + (1 - x_3)\phi_K^A(\bar{x}_2)] \cdot E_e'(t_b) h_n(x_1, x_2, 1 - x_3, b_1, b_3) \\ & + [-(x_2 + x_3)\phi_K^A(\bar{x}_2) + r_K x_2(\phi_K^P(\bar{x}_2) - \phi_K^T(\bar{x}_2))] \\ & \cdot E_e'(t_b') h_n(x_1, x_2, x_3, b_1, b_3)\}, \end{aligned} \tag{34}$$

where ϕ_η denotes ϕ_{η_q} or ϕ_{η_s}.

There are two kinds of contributions from $(V - A) \times (V + A)$ operators: M_{eK}^{P1} and M_{eK}^{P2}, corresponding to the $(V - A)(V + A)$ and $(S - P)(S + P)$ type operators respectively:

$$\begin{aligned} M_{eK}^{P1} = {} & \frac{16}{\sqrt{3}}\pi G_F C_F m_B^4 \int_0^1 dx_1 dx_2 dx_3 \int_0^\infty b_1 db_1 b_3 db_3 \phi_B(x_1, b_1) \cdot \{[(1 - x_3)\phi_K^A(\bar{x}_2)(\phi_\eta^P(\bar{x}_3) - \phi_\eta^T(\bar{x}_3)) \\ & + r_K(1 - x_3)(\phi_K^P(\bar{x}_2) + \phi_K^T(\bar{x}_2))(\phi_\eta^P(\bar{x}_3) - \phi_\eta^T(\bar{x}_3)) + r_K x_2(\phi_K^P(\bar{x}_2) - \phi_K^T(\bar{x}_2))(\phi_\eta^P(\bar{x}_3) + \phi_\eta^T(\bar{x}_3))] \\ & \cdot E_e'(t_b) h_n(x_1, x_2, 1 - x_3, b_1, b_3) - [x_3\phi_K^A(\bar{x}_2)(\phi_\eta^P(\bar{x}_3) + \phi_\eta^T(\bar{x}_3)) + r_2 x_3(\phi_K^P(\bar{x}_2) + \phi_K^T(\bar{x}_2))(\phi_\eta^P(\bar{x}_3) \\ & + \phi_\eta^T(\bar{x}_3)) + r_2 x_2(\phi_K^P(\bar{x}_2) - \phi_K^T(\bar{x}_2))(\phi_\eta^P(\bar{x}_3) - \phi_\eta^T(\bar{x}_3))] \cdot E_e'(t_b') h_n(x_1, x_2, x_3, b_1, b_3)\}, \end{aligned} \tag{35}$$

$$M_{eK}^{P2} = \frac{16}{\sqrt{3}}\pi G_F C_F m_B^4 \int_0^1 dx_1 dx_2 dx_3 \int_0^\infty b_1 db_1 b_3 db_3 \phi_B(x_1, b_1)\phi_\eta^A(\bar{x}_3)\cdot\{[-(1+x_2-x_3)\phi_K^A(\bar{x}_2) + x_2 r_K(\phi_K^P(\bar{x}_2) - \phi_K^T(\bar{x}_2))]\cdot E_e'(t_b)h_n(x_1, x_2, 1-x_3, b_1, b_3) + [x_3\phi_K^A(\bar{x}_2) - x_2 r_K(\phi_K^P(\bar{x}_2) + \phi_K^T(\bar{x}_2))]\cdot E_e'(t_b')h_n(x_1, x_2, x_3, b_1, b_3)\}. \tag{36}$$

For the nonfactorizable annihilation diagrams (Figs. 1(e) and 1(f)) again all three wave functions are involved. Here we have two kinds of contributions: $M_{aK}^{P2} = 0$, M_{aK}, and M_{aK}^{P1} describe the contributions from the $(V-A)(V-A)$ and $(V-A)(V+A)$ type operators, respectively,

$$M_{aK} = \frac{16}{\sqrt{3}}\pi G_F C_F m_B^4 \int_0^1 dx_1 dx_2 dx_3 \int_0^\infty b_1 db_1 b_3 db_3 \phi_B(x_1, b_1)\cdot\{[(1-x_2)\phi_K^A(\bar{x}_2)\phi_\eta^A(\bar{x}_3) + r_K r_\eta(1-x_2)(\phi_K^P(\bar{x}_2) + \phi_K^T(\bar{x}_2))(\phi_\eta^P(\bar{x}_3) - \phi_\eta^T(\bar{x}_3)) + r_K r_\eta x_3(\phi_K^P(\bar{x}_2) - \phi_K^T(\bar{x}_2))(\phi_\eta^P(\bar{x}_3) + \phi_\eta^T(\bar{x}_3))]\cdot E_a'(t_c)h_{na}(x_1, x_2, x_3, b_1, b_3) - [x_3\phi_K^A(\bar{x}_2)\phi_\eta^A(\bar{x}_3) + 4r_K r_\eta\phi_K^P(\bar{x}_2)\phi_\eta^P(\bar{x}_3) - r_K r_\eta(1-x_3)(\phi_K^P(\bar{x}_2) + \phi_K^T(\bar{x}_2))\cdot(\phi_\eta^P(\bar{x}_3) - \phi_\eta^T(\bar{x}_3)) - r_K r_\eta x_2(\phi_K^P(\bar{x}_2) - \phi_K^T(\bar{x}_2))(\phi_\eta^P(\bar{x}_3) + \phi_\eta^T(\bar{x}_3))]\cdot E_a'(t_c')h_{na}(x_1, x_2, x_3, b_1, b_3)\}, \tag{37}$$

$$M_{aK}^{P1} = \frac{16}{\sqrt{3}}\pi G_F C_F m_B^4 \int_0^1 dx_1 dx_2 dx_3 \int_0^\infty b_1 db_1 b_3 db_3 \phi_B(x_1, b_1)\{[-(1-x_2)r_K\phi_\eta^A(\bar{x}_3)(\phi_K^P(\bar{x}_2) + \phi_K^T(\bar{x}_2)) + r_\eta x_3\phi_K^A(\bar{x}_2)(\phi_\eta^P(\bar{x}_3) - \phi_\eta^T(\bar{x}_3))]E_a'(t_c)h_{na}(x_1, x_2, x_3, b_1, b_3) - [(x_2+1)r_K\phi_\eta^A(\bar{x}_3)(\phi_K^P(\bar{x}_2) + \phi_K^T(\bar{x}_2)) + r_\eta(x_3-2)\phi_K^A(\bar{x}_2)(\phi_\eta^P(\bar{x}_3) - \phi_\eta^T(\bar{x}_3))]E_a'(t_c')h_{na}(x_1, x_2, x_3, b_1, b_3)\}. \tag{38}$$

The factorizable annihilation diagrams (Figs. 1(g) and 1(h)) involve only K and $\eta^{(\prime)}$ wave functions. There are also three kinds of decay amplitudes for these two diagrams.,F_{aK}, F_{aK}^{P1} and F_{aK}^{P2}:

$$F_{aK} = F_{aK}^{P1} = \frac{8}{\sqrt{2}}\pi G_F C_F m_B^4 \int_0^1 dx_2 dx_3 \int_0^\infty b_2 db_2 b_3 db_3\{-[(1-x_2)\phi_K^A(\bar{x}_2)\phi_\eta^A(\bar{x}_3) + 4r_\eta r_K\phi_K^P(\bar{x}_2)\phi_\eta^P(\bar{x}_3) - 2r_K r_\eta x_2\phi_\eta^P(\bar{x}_3)(\phi_K^P(\bar{x}_2) + \phi_K^T(\bar{x}_2))]\cdot E_a(t_d)h_a(x_3, 1-x_2, b_3, b_2) + [x_3\phi_K^A(\bar{x}_2)\phi_\eta^A(\bar{x}_3) + 2r_\eta r_K\phi_K^P(\bar{x}_2)(\phi_\eta^P(\bar{x}_3) + \phi_\eta^T(\bar{x}_3)) + 2r_\eta r_K x_3\phi_K^P(\bar{x}_2)(\phi_\eta^P(\bar{x}_3) - \phi_\eta^T(\bar{x}_3))]\cdot E_a(t_d')h_a(1-x_2, x_3, b_2, b_3)\}, \tag{39}$$

$$F_{aK}^{P2} = \frac{16}{\sqrt{2}}\pi G_F C_F m_B^4 \int_0^1 dx_2 dx_3 \int_0^\infty b_2 db_2 b_3 db_3\cdot\{[r_K(1-x_2)(\phi_K^P(\bar{x}_2) - \phi_K^T(\bar{x}_2))\phi_\eta^A(\bar{x}_3) + 2r_\eta\phi_K^A(\bar{x}_2)\phi_\eta^P(\bar{x}_3)]\cdot E_a(t_d)h_a(x_3, 1-x_2, b_3, b_2) + [2r_K\phi_K^P(\bar{x}_2)\phi_\eta^A(\bar{x}_3) + x_3 r_\eta\phi_K^A(\bar{x}_2)(\phi_\eta^P(\bar{x}_3) + \phi_\eta^T(\bar{x}_3))]\cdot E_a(t_d')h_a(1-x_2, x_3, b_2, b_3)\}. \tag{40}$$

The evolution function $E_i(t_j)$ and hard function h_i appeared in Eqs. (33)–(40) and are given explicitly in the Appendix.

If we exchange the K and $\eta^{(\prime)}$ in Fig. 1, the corresponding decay amplitudes for new diagrams will be similar with those as given in Eqs. (31)–(40), since the K and $\eta^{(\prime)}$ are all pseudoscalar mesons and have similar wave functions. The decay amplitudes for new diagrams, say $F_{e\eta}$, $F_{e\eta}^{P1,P2}$, $M_{e\eta}$, $M_{e\eta}^{P1,P2}$, $M_{a\eta}$,$M_{a\eta}^{P1}$, $F_{a\eta}$,$F_{a\eta}^{P1,P2}$, can be obtained from those as given in Eqs. (31)–(40) by the following replacements:

$$\phi_K^A \leftrightarrow \phi_{\eta^{(\prime)}}^A, \qquad \phi_K^P \leftrightarrow \phi_{\eta^{(\prime)}}^P, \qquad \phi_K^T \leftrightarrow \phi_{\eta^{(\prime)}}^T, \qquad r_K \leftrightarrow r_{\eta^{(\prime)}}. \tag{41}$$

For $B^0 \to K^0\eta$ decay, by combining the contributions from all possible configurations of Feynman diagrams, one finds the total decay amplitude with the inclusion of the corresponding Wilson coefficients as follows:

$$\begin{aligned}\mathcal{M}(K^0\eta) &= \langle K^0\eta|H_{\rm eff}|B^0\rangle \\ &= F_{eK}\Big\{\Big[\xi_u a_2 - \xi_t\Big(2a_3 - 2a_5 - \frac{1}{2}a_7 + \frac{1}{2}a_9\Big)\Big]f_\eta^q - \xi_t\Big(a_3 + a_4 - a_5 + \frac{1}{2}a_7 - \frac{1}{2}a_9 - \frac{1}{2}a_{10}\Big)f_\eta^s\Big\} \\ &\quad - F_{e\eta}\xi_t\Big(a_4 - \frac{1}{2}a_{10}\Big)f_K F_1(\phi) - [F_{eK}^{P_2} f_\eta^s + F_{e\eta}^{P_2} f_K F_1(\phi)]\xi_t\Big(a_6 - \frac{1}{2}a_8\Big) - [F_{ak}F_2(\phi) + F_{a\eta}F_1(\phi)] \\ &\quad \times \xi_t\Big(a_4 - \frac{1}{2}a_{10}\Big) + [F_{aK}^{P_2}F_2(\phi) + F_{a\eta}^{P_2}F_1(\phi)]\xi_t\Big(a_6 - \frac{1}{2}a_8\Big)f_B + M_{eK}\Big\{\Big[\xi_u C_2 - \xi_t\cdot\Big(2C_4 + \frac{1}{2}C_{10}\Big)\Big]F_1(\phi) \\ &\quad - \xi_t\Big(C_3 + C_4 - \frac{1}{2}C_9 - \frac{1}{2}C_{10}\Big)F_2(\phi)\Big\} - M_{e\eta}\xi_t\Big(C_3 - \frac{1}{2}C_9\Big)F_1(\phi) - [M_{eK}^{P1}F_2(\phi) + M_{e\eta}^{P1}F_1(\phi)] \\ &\quad \times \xi_t\Big(C_5 - \frac{1}{2}C_7\Big) - M_{eK}^{P_2}\xi_t\Big[\Big(2C_6 + \frac{1}{2}C_8\Big)F_1(\phi) + (C_6 - \frac{1}{2}C_8)F_2(\phi)\Big] \end{aligned} \tag{42}$$

where $\xi_u = V_{ub}^* V_{us}$, $\xi_t = V_{tb}^* V_{ts}$, and $F_1(\phi)$, $F_2(\phi)$ are the mixing factors as given in Eq. (22).

The coefficients a_i in Eq. (42) are the combinations of the Wilson coefficients C_i, and have been defined as usual:

$$\begin{aligned} a_1 = C_2 + \frac{C_1}{3}, \qquad a_2 = C_1 + \frac{C_2}{3}, \qquad a_i = C_i + \frac{C_{i+1}}{3}, \quad \text{for } i = 3, 5, 7, 9, \\ a_i = C_i + \frac{C_{i-1}}{3}, \quad \text{for } i = 4, 6, 8, 10. \end{aligned} \tag{43}$$

Similarly, the decay amplitude for $B^+ \to K^+\eta$ can be written as

$$\begin{aligned}\mathcal{M}(K^+\eta) &= \langle K^+\eta|H_{\rm eff}|B^0\rangle \\ &= F_{eK}\Big\{\Big[\xi_u a_2 - \xi_t\Big(2a_3 - 2a_5 - \frac{1}{2}a_7 + \frac{1}{2}a_9\Big)\Big]f_\eta^q - \xi_t\Big(a_3 + a_4 - a_5 + \frac{1}{2}a_7 - \frac{1}{2}a_9 - \frac{1}{2}a_{10}\Big)f_\eta^s\Big\} \\ &\quad + [F_{e\eta}F_1(\phi)f_K + (F_{a\eta}F_1(\phi) + F_{aK}F_2(\phi))f_B]\xi_u a_1 - [F_{e\eta}F_1(\phi)f_K + (F_{a\eta}F_1(\phi) + F_{aK}F_2(\phi))f_B] \\ &\quad \times \xi_t(a_4 + a_{10}) - [F_{e\eta}^{P2}F_1(\phi)f_K + (F_{a\eta}^{P2}F_1(\phi) + F_{aK}^{P2}F_2(\phi))f_B]\xi_t(a_6 + a_8) - F_{eK}^{P2}f_\eta^s\xi_t\Big(a_6 - \frac{1}{2}a_8\Big) \\ &\quad - M_{eK}^{P1}\xi_t\Big(C_5 - \frac{1}{2}C_7\Big) + M_{eK}\Big\{\Big[\xi_u C_2 - \xi_t\Big(2C_4 + \frac{1}{2}C_{10}\Big)\Big]F_1(\phi) - \xi_t\Big(C_3 + C_4 - \frac{1}{2}C_9 - \frac{1}{2}C_{10}\Big)F_2(\phi)\Big\} \\ &\quad + [M_{aK}F_2(\phi) + (M_{e\eta} + M_{a\eta})F_1(\phi)][\xi_u C_1 - \xi_t(C_3 + C_9)] - [M_{aK}^{P1}F_2(\phi) + (M_{e\eta}^{P1} + M_{a\eta}^{P1})F_1(\phi)] \\ &\quad \times \xi_t(C_5 + C_7) - M_{eK}^{P2}\xi_t\Big[\Big(2C_6 + \frac{1}{2}C_8\Big)F_1(\phi) + (C_6 - \frac{1}{2}C_8)F_2(\phi)\Big]. \end{aligned} \tag{44}$$

The total decay amplitude for $B^0 \to K^0\eta'$ and $B^+ \to K^+\eta'$ can be obtained easily from Eqs. (42) and (44) by the following replacements:

$$\begin{aligned} f_\eta^d \to f_{\eta'}^d, \qquad f_\eta^s \to f_{\eta'}^s, \qquad F_1(\phi) \to F_1^l(\phi), \\ F_2(\phi) \to F_2^l(\phi). \end{aligned} \tag{45}$$

IV. NLO CONTRIBUTIONS IN PQCD APPROACH

A. General discussion

The power counting in the pQCD factorization approach [25] is different from that in the QCD factorization [14,17]. When compared with the previous LO calculations in pQCD [18,30,31], the following NLO contributions should be considered:

(1) The LO Wilson coefficients $C_i(m_W)$ will be replaced by those at NLO level in the NDR scheme [32], and the NLO RG evolution matrix $U(t, m, \alpha)$ instead of $U(m_1, m_2)^{(0)}$, as defined in Ref. [32], will be used here:

$$U(m_1, m_2, \alpha) = U(m_1, m_2) + \frac{\alpha}{4\pi}R(m_1, m_2) \tag{46}$$

where the function $U(m_1, m_2)$ and $R(m_1, m_2)$ represent the QCD and QED evolution and have been defined in Eq. (6.24) and (7.22) in Ref. [32]. We also introduce a cutoff $\mu_0 = 1.0$ GeV for the QCD running of $C_i(t)$ in the final integration.

(2) The strong coupling constant $\alpha_s(t)$ at two-loop level as given in Eq. (10) will be used.

(3) Besides the LO hard kernel $H^{(0)}(\alpha_s)$, the NLO hard kernel $H^{(1)}(\alpha_s^2)$ should be included. All the Feynman diagrams, which lead to the decay amplitudes proportional to $\alpha_s^2(t)$, should be considered. Such Feynman diagrams can be grouped into following classes:

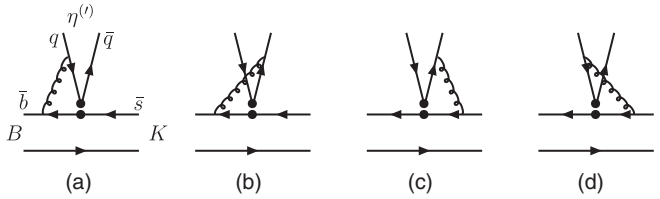

FIG. 2. NLO vertex corrections to the factorizable amplitudes.

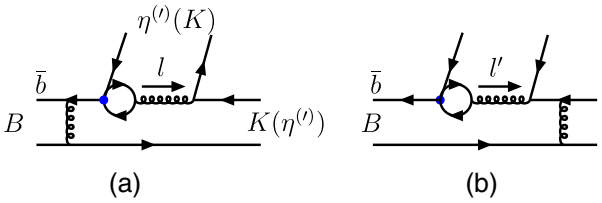

FIG. 3 (color online). Quark-loop amplitudes.

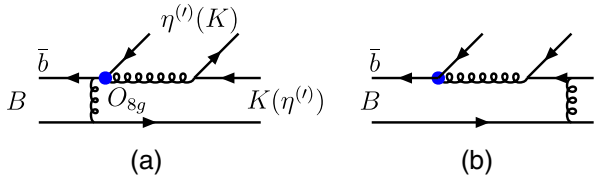

FIG. 4 (color online). Chromomagnetic penguin amplitudes (O_{8g}). There are nine relevant Feynman diagrams as shown in Ref. [38]. Here we show the first two only, which provide dominant contribution of such diagrams.

(I) The vertex corrections, as illustrated in Fig. 2, the same set as that studied in the QCDF approach.

(II) The NLO contributions from quark-loops, as illustrated in Fig. 3.

(III) The NLO contributions from chromomagnetic penguins, i.e. the operator O_{8g}, as illustrated in Fig. 4. There are a total of nine relevant Feynman diagrams as given in Ref. [38], if the Feynman diagrams involving the three-gluon vertex are also included. We here show the first two only, and they provide the dominant NLO contributions, according to Ref. [38].

(IV) The NLO contributions to the Feynman diagrams (Figs. 1(a) and 1(b)) corresponding to the extraction of factors, as illustrated in Fig. 5. There area total of 13 relevant Feynman diagrams We here show four of them only.

(V) The NLO contributions to the hard-spectator Feynman diagrams (Figs. 1(c) and 1(d)) as illustrated in Fig. 6. There are a total of 56 relevant Feynman diagrams We here show four only.

(VI) The NLO contributions to the annihilation Feynman diagrams (Figs. 1(e) and 1(h)) as illustrated in Fig. 7. We here show only four such diagrams.

For the last four classes (III–VI), the Feynman diagrams involving a three-gluon vertex should be included. At present, the calculations for the vertex corrections, the quark-loops and chromomagnetic penguins have been available and will be considered here. For the Feynman diagrams as shown in Figs. 5–7, however, the analytical calculations have not been completed yet. What we can do here is to include the NLO contributions to the hard kernel H.

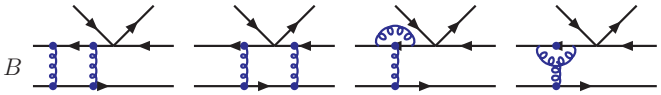

FIG. 5 (color online). The four typical Feynman diagrams, which contribute to the form factors at NLO level.

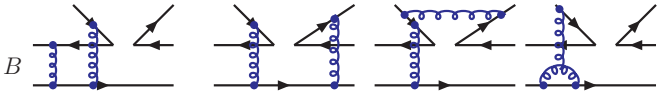

FIG. 6 (color online). The four typical hard-spectator Feynman diagrams, which contribute at NLO level.

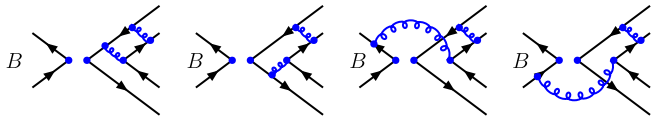

FIG. 7 (color online). The four typical annihilation Feynman diagrams, which contribute at NLO level.

B. Vertex corrections

The vertex corrections to the factorizable emission diagrams, as illustrated by Fig. 2, were calculated years ago in the QCD factorization approach [14,15,17].

For the emission diagram, there are four kinds of single gluon exchange responsible for the effective vertex as labeled in Fig. 2. The contributions from the soft gluons and collinear gluons are power suppressed, that is to say the total contributions of these four figures are infrared finite. For charmless B meson decays, these corrections can be calculated without considering the transverse momentum effects of the quark at the end-point in the collinear factorization theorem. Therefore, there is no need to employ the k_T factorization theorem. In fact, the difference of the calculations induced by considering or not considering the parton transverse momentum is rather small [25], say less than 10%, and therefore can be neglected. Consequently, one can use the vertex corrections as given in Ref. [15] directly. The vertex corrections can then be absorbed into the redefinition of the Wilson coefficients $a_i(\mu)$ by adding a vertex-function $V_i(M)$ to them [15,17]

$$a_i(\mu) \to a_i(\mu) + \frac{\alpha_s(\mu)}{4\pi} C_F \frac{C_i(\mu)}{3} V_i(M), \quad \text{for } i = 1, 2;$$
$$a_j(\mu) \to a_j(\mu) + \frac{\alpha_s(\mu)}{4\pi} C_F \frac{C_{j+1}(\mu)}{3} V_j(M), \quad \text{for } j = 3, 5, 7, 9,$$
$$a_j(\mu) \to a_j(\mu) + \frac{\alpha_s(\mu)}{4\pi} C_F \frac{C_{j-1}(\mu)}{3} V_j(M), \quad \text{for } j = 4, 6, 8, 10, \tag{47}$$

where M is the meson emitted from the weak vertex. When M is a pseudoscalar meson, the vertex functions $V_i(M)$ are given (in the NDR scheme) in Refs. [15,25]:

$$V_i(M) = \begin{cases} 12\ln\frac{m_b}{\mu} - 18 + \frac{2\sqrt{6}}{f_M}\int_0^1 dx \phi_M^A(x) g(x), & \text{for } i = 1-4, 9, 10, \\ -12\ln\frac{m_b}{\mu} + 6 - \frac{2\sqrt{6}}{f_M}\int_0^1 dx \phi_M^A(x) g(1-x), & \text{for } i = 5, 7, \\ -6 + \frac{2\sqrt{6}}{f_M}\int_0^1 dx \phi_M^P(x) h(x), & \text{for } i = 6, 8, \end{cases} \tag{48}$$

where f_M is the decay constant of the meson M; $\phi_M^A(x)$ and $\phi_M^P(x)$ are the twist-2 and twist-3 distribution amplitude of the meson M, respectively. The hard-scattering functions $g(x)$ and $h(x)$ in Eq. (48) are

$$g(x) = 3\left(\frac{1-2x}{1-x}\ln x - i\pi\right) + \left[2\mathrm{Li}_2(x) - \ln^2 x + \frac{2\ln x}{1-x} - (3 + 2i\pi)\ln x - (x \leftrightarrow 1-x)\right], \tag{49}$$

$$h(x) = 2\mathrm{Li}_2(x) - \ln^2 x - (1 + 2i\pi)\ln x - (x \leftrightarrow 1-x), \tag{50}$$

where $\mathrm{Li}_2(x)$ is the dilogarithm function. As shown in Ref. [25], the μ-dependence of the Wilson coefficients $a_i(\mu)$ will be improved generally by the inclusion of the vertex corrections.

C. Quark loops

The contribution from the so-called "quark loops" is a kind of penguin correction with the four quark operators insertion, as illustrated by Fig. 3. In fact this is generally called the BSS mechanism [39], which provides the strong phase needed to induce the CP violation in the QCDF approach. We here include quark-loop amplitude from the operators $O_{1,2}$ and O_{3-6} only. The quark loops from O_{7-10} will be neglected due to their smallness.

For the $b \to s$ transition, the contributions from the various quark loops are given by

$$H_{\mathrm{eff}}^{(\mathrm{ql})} = -\sum_{q=u,c,t}\sum_{q'}\frac{G_F}{\sqrt{2}} V_{qb}V_{qs}^* \frac{\alpha_s(\mu)}{2\pi} C^q(\mu, l^2) \times (\bar{s}\gamma_\rho(1-\gamma_5)T^a b)(\bar{q}'\gamma^\rho T^a q'), \tag{51}$$

where l^2 is the invariant mass of the gluon, which attaches the quark loops in Fig. 3. The functions $C^q(\mu, l^2)$ are written as

$$C^q(\mu, l^2) = \left[G^q(\mu, l^2) - \frac{2}{3}\right]C_2(\mu), \tag{52}$$

for $q = u, c$ and

$$C^{(t)}(\mu, l^2) = \left[G^{(s)}(\mu, l^2) - \frac{2}{3}\right]C_3(\mu) + \sum_{q''=u,d,s,c} G^{(q'')}(\mu, l^2)[C_4(\mu) + C_6(\mu)]. \tag{53}$$

The function $G^{(q)}(\mu, l^2)$ for the loop of the quark $q(q = u, d, s, c)$ is given by [25]

$$G^{(q)}(\mu, l^2) = -4\int_0^1 dx x(1-x)\ln\frac{m_q^2 - x(1-x)l^2}{\mu^2}; \tag{54}$$

m_q is the possible quark mass. The explicit expressions of the function $G^{(q)}(\mu, l^2)$ after the integration can be found, for example, in Ref. [25].

It is straightforward to calculate the decay amplitude for Figs. 3(a) and 3(b). We find two kinds of topological decay amplitudes:

$$M_{K\eta_s}^{(q)} = -\frac{8}{\sqrt{6}} C_F^2 m_B^4 \int_0^1 dx_1 dx_2 dx_3 \int_0^\infty b_1 db_1 b_2 db_2 \phi_B(x_1, b_1) \cdot \{[(1+x_2)\phi_K^A(\bar{x}_2)\phi_{\eta_s}^A(\bar{x}_3) + r_K(1-2x_2)(\phi_K^P(\bar{x}_2) - \phi_K^T(\bar{x}_2))\phi_{\eta_s}^A(\bar{x}_3) + 2r_{\eta_s}\phi_K^A(\bar{x}_2)\phi_{\eta_s}^P(\bar{x}_3) + 2r_K r_{\eta_s}((2+x_2)\phi_K^P(\bar{x}_2) + x_2\phi_K^T(\bar{x}_2))\phi_{\eta_s}^P(\bar{x}_3)] \cdot E^{(q)}(t_q, l^2)h_e(x_2, x_1, b_2, b_1) + [2r_K\phi_K^P(\bar{x}_2)\phi_{\eta_s}^A(\bar{x}_3) + 4r_K r_{\eta_s}\phi_K^P(\bar{x}_2)\phi_{\eta_s}^P(\bar{x}_3)] \cdot E^{(q)}(t_q', l'^2)h_e(x_1, x_2, b_1, b_2)\}, \tag{55}$$

for $B \to K$ transition, and

$$M^{(q)}_{\eta_q K} = -\frac{8}{\sqrt{6}} C_F^2 m_B^4 \int_0^1 dx_1 dx_2 dx_3 \int_0^\infty b_1 db_1 b_2 db_2 \phi_B(x_1, b_1) \cdot \{[(1+x_2)\phi^A_{\eta_q}(\bar{x}_2)\phi^A_K(\bar{x}_3) + r_\eta(1-2x_2) \times (\phi^P_{\eta_q}(\bar{x}_2) - \phi^T_{\eta_q}(\bar{x}_2))\phi^A_K(\bar{x}_3) + 2r_K\phi^A_{\eta_q}(\bar{x}_2)\phi^P_K(\bar{x}_3) + 2r_\eta r_K((2+x_2)\phi^P_{\eta_q}(\bar{x}_2) + x_2\phi^T_{\eta_q}(\bar{x}_2))\phi^P_K(\bar{x}_3)] \cdot E^{(q)}(t_q, l^2) h_e(x_2, x_1, b_2, b_1) + [2r_\eta\phi^P_{\eta_q}(\bar{x}_2)\phi^A_K(\bar{x}_3) + 4r_\eta r_K\phi^P_{\eta_q}(\bar{x}_2)\phi^P_K(\bar{x}_3)] \cdot E^{(q)}(t'_q, l'^2) h_e(x_1, x_2, b_1, b_2)\}, \quad (56)$$

for $B \to \eta$ transition. Here $r_\eta = m_0^q/m_B$ and $r_{\eta_s} = m_0^s/m_B$. The evolution factors in Eqs. (55) and (56) take the form of

$$E^{(q)}(t, l^2) = C^{(q)}(t, l^2)\alpha_s^2(t) \cdot \exp[-S_{ab}], \quad (57)$$

with the Sudakov factor S_{ab} and the hard function $h_e(x_1, x_2, b_1, b_2)$ as given in Eqs. (A2) and (A9) respectively, and finally the hard scales and the gluon invariant masses are

$$t_q = \max(\sqrt{x_2}m_B, \sqrt{x_1x_2}m_B, \sqrt{(1-x_2)x_3}m_B, 1/b_1, 1/b_2),$$
$$t'_q = \max(\sqrt{x_1}m_B, \sqrt{x_1x_2}m_B, \sqrt{|x_3-x_1|}m_B, 1/b_1, 1/b_2), \quad (58)$$

$$l^2 = (1-x_2)x_3m_B^2 - |\mathbf{k}_{2\mathrm{T}} - \mathbf{k}_{3\mathrm{T}}|^2 \approx (1-x_2)x_3m_B^2,$$
$$l'^2 = (x_3-x_1)m_B^2 - |\mathbf{k}_{1\mathrm{T}} - \mathbf{k}_{3\mathrm{T}}|^2 \approx (x_3-x_1)m_B^2. \quad (59)$$

For $B \to K\eta'$ decays, we find the same decay amplitude. Finally, the total "quark-loop" contribution to the considered $B \to K\eta^{(\prime)}$ ($K = K^0, K^+$) decays can be written as

$$M^{(\mathrm{ql})}_{K\eta} = \langle K\eta|\mathcal{H}^{\mathrm{ql}}_{\mathrm{eff}}|B\rangle = \frac{G_F}{\sqrt{2}}\sum_{q=u,c,t}\lambda_q[M^{(q)}_{K\eta_s}F_2(\phi) + M^{(q)}_{\eta_q K}F_1(\phi)], \quad (60)$$

$$M^{(\mathrm{ql})}_{K\eta'} = \langle K\eta'|\mathcal{H}^{(\mathrm{ql})}_{\mathrm{eff}}|B\rangle = \frac{G_F}{\sqrt{2}}\sum_{q=u,c,t}\lambda_q[M^{(q)}_{K\eta_s}F'_2(\phi) + M^{(q)}_{\eta_q K}F'_1(\phi)], \quad (61)$$

where $\lambda_q = V_{qb}V^*_{qs}$. The mixing parameters $F_1(\phi)$, $F'_1(\phi)$, $F_2(\phi)$ and $F'_2(\phi)$ have been defined in Eqs. (22).

It is worth noting that the quark-loop corrections are mode dependent. The assumption of a constant gluon invariant mass in FA introduces a large theoretical uncertainty in making predictions. In the pQCD approach, however, the gluon invariant mass is related to the parton momenta unambiguously and will disappear after the integration.

D. Magnetic penguins

This is another kind of penguin correction but with the magnetic-penguin operator insertion. The corresponding weak effective Hamiltonian contains the $b \to sg$ transition,

$$H^{\mathrm{cmp}}_{\mathrm{eff}} = -\frac{G_F}{\sqrt{2}}V_{tb}V^*_{ts}C^{\mathrm{eff}}_{8g}O_{8g}, \quad (62)$$

with the chromomagnetic penguin operator,

$$O_{8g} = \frac{g_s}{8\pi^2}m_b\bar{d}_i\sigma^{\mu\nu}(1+\gamma_5)T^a_{ij}G^a_{\mu\nu}b_j, \quad (63)$$

where i, j are the color indices of quarks. The corresponding effective Wilson coefficient $C^{\mathrm{eff}}_{8g} = C_{8g} + C_5$ [25].

The decay amplitudes obtained by evaluating the Feynman diagrams, Fig. 4(a) and 4(b), can be written as

$$M^{(g)}_{K\eta_s} = \frac{8}{\sqrt{6}}C_F^2m^6\int_0^1 dx_1dx_2dx_3\int_0^\infty b_1db_1b_2db_2\phi_B(x_1,b_1)\cdot\{\{-(1-x_2)[2\phi^A_K(\bar{x}_2) + r_K(3\phi^P_K(\bar{x}_2) - \phi^T_K(\bar{x}_2)) + r_Kx_2(\phi^P_K(\bar{x}_2) + \phi^T_K(\bar{x}_2))]\phi^A_{\eta_s}(\bar{x}_3) - r_{\eta_s}(1+x_2)x_3\phi^A_K(\bar{x}_2)(3\phi^P_{\eta_s}(\bar{x}_3) + \phi^T_{\eta_s}(\bar{x}_3)) - r_Kr_{\eta_s}(1-x_2)(\phi^P_K(\bar{x}_2) + \phi^T_K(\bar{x}_2))(3\phi^P_{\eta_s}(\bar{x}_3) - \phi^T_{\eta_s}(\bar{x}_3)) - r_Kr_{\eta_s}x_3(1-2x_2)(\phi^P_K(\bar{x}_2) - \phi^T_K(\bar{x}_2))(3\phi^P_{\eta_s}(\bar{x}_3) + \phi^T_{\eta_s}(\bar{x}_3))\} \cdot E_g(t_q)h_g(A,B,C,b_1,b_2,b_3,x_2) - [4r_K\phi^P_K(\bar{x}_2)\phi^A_{\eta_s}(\bar{x}_3) + 2r_Kr_{\eta_s}x_3\phi^P_K(\bar{x}_2)(3\phi^P_{\eta_s}(\bar{x}_3) + \phi^T_{\eta_s}(\bar{x}_3))] \cdot E_g(t'_q)h_g(A',B',C',b_2,b_1,b_3,x_1)\}, \quad (64)$$

$$M^{(g)}_{\eta_q K} = \frac{8}{\sqrt{6}}C_F^2m^6\int_0^1 dx_1dx_2dx_3\int_0^\infty b_1db_1b_2db_2\phi_B(x_1,b_1)\cdot\{\{-(1-x_2)[2\phi^A_{\eta_q}(\bar{x}_2) + r_\eta(3\phi^P_{\eta_q}(\bar{x}_2) - \phi^T_{\eta_q}(\bar{x}_2)) + r_\eta x_2(\phi^P_{\eta_q}(\bar{x}_2) + \phi^T_{\eta_q}(\bar{x}_2))]\phi^A_K(\bar{x}_3) - r_K(1+x_2)x_3\phi^A_{\eta_q}(\bar{x}_2)(3\phi^P_K(\bar{x}_3) + \phi^T_K(\bar{x}_3)) - r_\eta r_K(1-x_2)(\phi^P_{\eta_q}(\bar{x}_2) + \phi^T_{\eta_q}(\bar{x}_2))(3\phi^P_K(\bar{x}_3) - \phi^T_K(\bar{x}_3)) - r_\eta r_Kx_3(1-2x_2)(\phi^P_{\eta_q}(\bar{x}_2) - \phi^T_{\eta_q}(\bar{x}_2))(3\phi^P_K(\bar{x}_3) + \phi^T_K(\bar{x}_3))\} \cdot E_g(t_q)h_g(A,B,C,b_1,b_2,b_3,x_2) - [4r_\eta\phi^P_{\eta_q}(\bar{x}_2)\phi^A_K(\bar{x}_3) + 2r_\eta r_Kx_3\phi^P_{\eta_q}(\bar{x}_2)(3\phi^P_K(\bar{x}_3) + \phi^T_K(\bar{x}_3))] \cdot E_g(t'_q)h_g(A',B',C',b_2,b_1,b_3,x_1)\}. \quad (65)$$

Here $r_\eta = m_0^q/m_B$, $r_{\eta_s} = m_0^s/m_B$. The evolution factors in Eqs. (64) and (65) take the form of

$$E^{(g)}(t, l^2) = \alpha_s^2(t) C_{8g}^{\rm eff}(t) \exp[-S_{mg}(t)], \tag{66}$$

with the Sudakov factor S_{mg}

$$\begin{aligned} S_{mg}(t) = {} & s(x_1 m_B/\sqrt{2}, b_1) + s(x_2 m_B/\sqrt{2}, b_2) \\ & + s((1-x_2) m_B/\sqrt{2}, b_2) + s(x_3 m_B/\sqrt{2}, b_3) \\ & + s((1-x_3) m_B/\sqrt{2}, b_3) - \frac{1}{\beta_1}\left[\ln\frac{\ln(t/\Lambda)}{-\ln(b_1\Lambda)}\right. \\ & \left. + \ln\frac{\ln(t/\Lambda)}{-\ln(b_2\Lambda)} + \ln\frac{\ln(t/\Lambda)}{-\ln(b_3\Lambda)}\right]. \end{aligned} \tag{67}$$

The hard function h_g in the chromomagnetic penguin amplitude is given by

$$\begin{aligned} h_g(A, B, C, b_1, b_2, b_3, x_i) = {} & -S_t(x_i) K_0(B b_1) K_0(C b_3) \\ & \times \int_0^{\pi/2} d\theta \tan\theta J_0(A b_1 \tan\theta) \\ & \times J_0(A b_2 \tan\theta) J_0(A b_3 \tan\theta) \end{aligned} \tag{68}$$

with the index $i = 1, 2$; the threshold resummation function $S_t(x_i)$ is given in Eq. (A7), and

$$\begin{aligned} & A = \sqrt{x_2} m_B, \quad B = B' = \sqrt{x_1 x_2} m_B, \quad C = i\sqrt{(1-x_2) x_3} m_B, \\ & A' = \sqrt{x_1} m_B, \quad B' = B, \quad C' = \sqrt{|x_1 - x_3|} m_B. \end{aligned} \tag{69}$$

Here the scale t_q, t_q', and the gluon invariant mass l^2 and l'^2 have been given in Eqs. (58) and (59).

Finally, the total chromomagnetic penguin contribution to the considered $B \to K\eta^{(\prime)}$ ($K = K^0, K^+$) decays can be written as

$$\begin{aligned} M_{K\eta}^{(\rm cmp)} &= \langle K\eta | \mathcal{H}_{\rm eff}^{\rm cmp} | B \rangle \\ &= -\frac{G_F}{\sqrt{2}} \lambda_t [M_{K\eta_s}^{(g)} F_2(\phi) + M_{\eta_q K}^{(g)} F_1(\phi)], \end{aligned} \tag{70}$$

$$\begin{aligned} M_{K\eta'}^{(\rm cmp)} &= \langle K\eta' | \mathcal{H}_{\rm eff}^{\rm cmp} | B \rangle \\ &= -\frac{G_F}{\sqrt{2}} \lambda_t [M_{K\eta_s}^{(g)} F_2'(\phi) + M_{\eta_q K}^{(g)} F_1'(\phi)]. \end{aligned} \tag{71}$$

The mixing parameters $F_1(\phi)$, $F_1'(\phi)$, $F_2(\phi)$ and $F_2'(\phi)$ have been defined in Eqs. (22) and (45).

V. NUMERICAL RESULTS AND DISCUSSIONS

A. Input parameters

We use the following input parameters [2,40] in the numerical calculations:

$$\begin{aligned} & f_B = 0.21 \text{ GeV}, \quad f_K = 0.16 \text{ GeV}, \\ & m_\eta = 547.5 \text{ MeV}, \quad m_{\eta'} = 957.8 \text{ MeV}, \\ & m_K = 0.49 \text{ GeV}, \quad m_{0K} = 1.7 \text{ GeV}, \\ & M_B = 5.279 \text{ GeV}, \quad m_b = 4.8 \text{ GeV}, \\ & M_W = 80.41 \text{ GeV}, \quad \tau_{B^0} = 1.527 \text{ ps}, \\ & \tau_{B^+} = 1.643 \text{ ps}. \end{aligned} \tag{72}$$

For the CKM quark-mixing matrix elements, we use the values as given in Refs. [2,40]:

$$\begin{aligned} & V_{ud} = 0.9745, \quad V_{us} = \lambda = 0.2200, \\ & |V_{ub}| = 4.31 \times 10^{-3}, \quad V_{cd} = -0.224, \\ & V_{cd} = 0.996, \quad V_{cb} = 0.0413, \\ & |V_{td}| = 7.4 \times 10^{-3}, \quad V_{ts} = -0.042, \\ & V_{tb} = 0.9991, \end{aligned} \tag{73}$$

with the CKM angles $\beta = 21.6°$, $\gamma = 60° \pm 20°$ and $\alpha = 100° \pm 20°$.

B. Branching ratios

Using the known wave functions and the central values of relevant input parameters, we find the LO pQCD predictions for the corresponding form factors at zero momentum transfer:

$$\begin{aligned} & F_0^{B\to\eta}(q^2 = 0) = 0.21 \pm 0.03(\omega_b), \\ & F_0^{B\to\eta'}(q^2 = 0) = 0.17 \pm 0.03(\omega_b), \\ & F_0^{B\to K}(q^2 = 0) = 0.37^{+0.06}_{-0.05}(\omega_b), \end{aligned} \tag{74}$$

for $\omega_b = 0.40 \pm 0.04$ GeV, which agree well with those obtained in QCD sum rule.

In the B-rest frame, the branching ratio of a general $B \to PP$ decay can be written as

$$\text{Br}(B \to M_2 M_3) = \tau_B \frac{1}{16\pi m_B} \chi |\mathcal{M}(B \to M_2 M_3)|^2, \tag{75}$$

where τ_B is the lifetime of the B meson, and χ is the phase space factor and will equal to one when the masses of final state light mesons are neglected. The total decay amplitude in Eq. (75) is defined as

$$\mathcal{M}(B \to M_2 M_3) = \langle M_2 M_3 | \mathcal{H}_{\rm eff} + \mathcal{H}_{\rm eff}^{\rm (ql)} + \mathcal{H}_{\rm eff}^{\rm (cmp)} | B \rangle. \tag{76}$$

Using the wave functions and the input parameters as specified in previous sections, it is straightforward to calculate the CP-averaged branching ratios for the considered four $B \to K\eta^{(\prime)}$ decays, which are listed in Table I. For comparison, we also list the corresponding updated experi-

TABLE I. The pQCD predictions for the branching ratios (in units of 10^{-6}). The label $\mathrm{LO}_{\mathrm{NLOWC}}$ means the LO results with the NLO Wilson coefficients, and +VC, +QL, +MP, NLO means the inclusion of the vertex corrections, the quark-loops, the magnetic penguin, and all the considered NLO corrections, respectively.

Mode	LO	$\mathrm{LO}_{\mathrm{NLOWC}}$	+VC	+QL	+MP	NLO	Data	QCDF
$B^+ \to K^+\eta$	4.7	4.7	4.3	4.9	3.1	3.2	2.6 ± 0.6	$1.9^{+3.0}_{-1.9}$
$B^+ \to K^+\eta'$	30.2	46.8	74.6	48.1	30.2	51.0	70.5 ± 3.5	$49.1^{+45.2}_{-23.6}$
$B^0 \to K^0\eta$	3.2	3.4	3.1	3.8	2.3	2.1	<2.0	$1.1^{+2.4}_{-1.5}$
$B^0 \to K^0\eta'$	31.3	46.5	69.7	48.5	20.7	50.3	68 ± 4	$46.5^{+41.9}_{-22.0}$

mental results [2] and numerical results evaluated in the framework of the QCDF approach [15].

It is worth stressing that the theoretical predictions in the pQCD approach have relatively large theoretical errors induced by the still large uncertainties of many input parameters, such as quark masses ($m_{u,d}, m_s$), chiral scales (m_{0K}, m_0^q, m_0^s), Gegenbauer coefficients ($a_i^{(K,\eta)}, \cdots$), ω_b and the CKM angles (α, γ), etc. The NLO pQCD predictions for the *CP*-averaged branching ratios with the major theoretical errors are the following:

$$\mathrm{Br}(B^+ \to K^+\eta) = [3.2^{+1.2}_{-0.9}(\omega_b)^{+2.7}_{-1.2}(m_s)^{+1.1}_{-1.0}(a_2^\eta)] \times 10^{-6}, \quad (77)$$

$$\mathrm{Br}(B^+ \to K^+\eta') = [51.0^{+13.5}_{-8.2}(\omega_b)^{+11.2}_{-6.2}(m_s)^{+4.2}_{-3.5}(a_2^\eta)] \times 10^{-6}, \quad (78)$$

$$\mathrm{Br}(B^0 \to K^0\eta) = [2.1^{+0.8}_{-0.6}(\omega_b)^{+2.3}_{-1.0}(m_s)^{+1.0}_{-0.9}(a_2^\eta)] \times 10^{-6}, \quad (79)$$

$$\mathrm{Br}(B^0 \to K^0\eta') = [50.3^{+11.8}_{-8.2}(\omega_b)^{+11.1}_{-6.2}(m_s)^{+4.5}_{-2.7}(a_2^\eta)] \times 10^{-6}. \quad (80)$$

The major errors are induced by the uncertainties of $\omega_b = 0.4 \pm 0.04$ GeV, $m_s = 130 \pm 30$ MeV and Gegenbauer coefficient $a_2^\eta = 0.44 \pm 0.22$ (here a_2^η denotes $a_2^{\eta_q}$ or $a_2^{\eta_s}$), respectively.

In Figs. 8 and 9, we show the parameter dependence of the pQCD predictions for the branching ratios of $B^+ \to K^+\eta^{(\prime)}$ and $B^0 \to K^0\eta^{(\prime)}$ decays for $\omega_b = 0.4 \pm 0.04$ GeV, $\gamma = [0°, 180°]$.

From the numerical results about the branching ratios, one can see that

(i) The decay amplitude $B \to K\eta_q$ and $B \to K\eta_s$ interfere constructively for $B \to K\eta'$ decays, but destructively for $B \to K\eta$ decays. This mechanism results in a factor of 6–10 disparity for the branching ratios of $B \to K^+\eta'$ and $B \to K^0\eta$ decays.

(ii) The LO pQCD predictions for branching ratios are much smaller (larger) than the measured values for $B \to K\eta'$ ($B \to K\eta$) decays, and show the same tendency as found in Ref. [16].

(iii) The NLO contributions can interfere constructively (destructively) with the corresponding LO part for

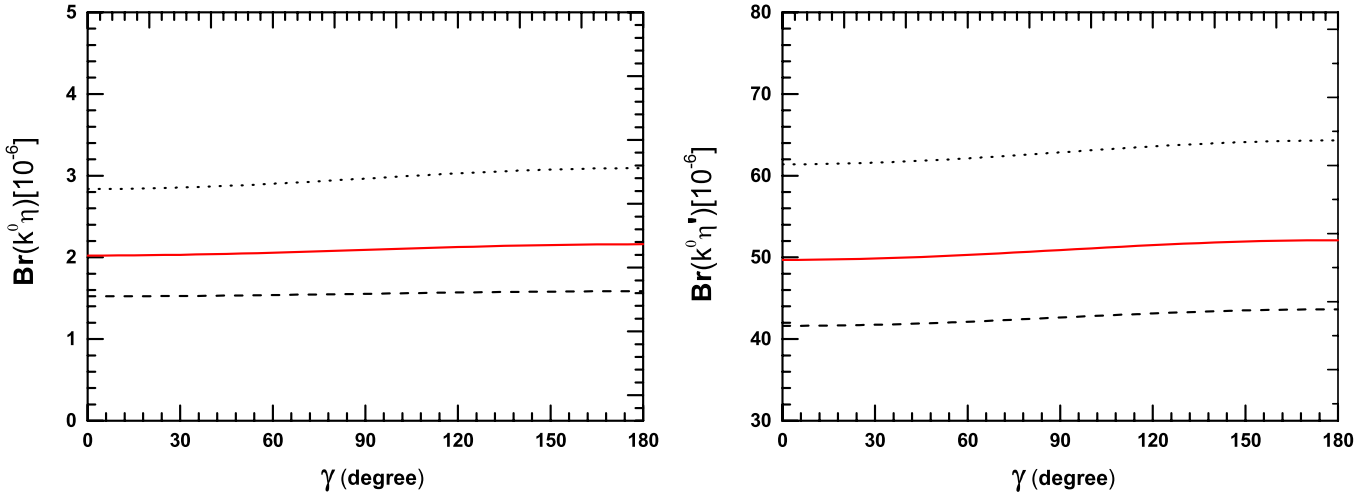

FIG. 8 (color online). The γ dependence of the branching ratios (in units of 10^{-6}) of $B^0 \to K^0\eta^{(\prime)}$ decays for $\omega_b = 0.36$ GeV (dotted curve), 0.40 GeV (solid curve), and 0.44 GeV (dashed curve).

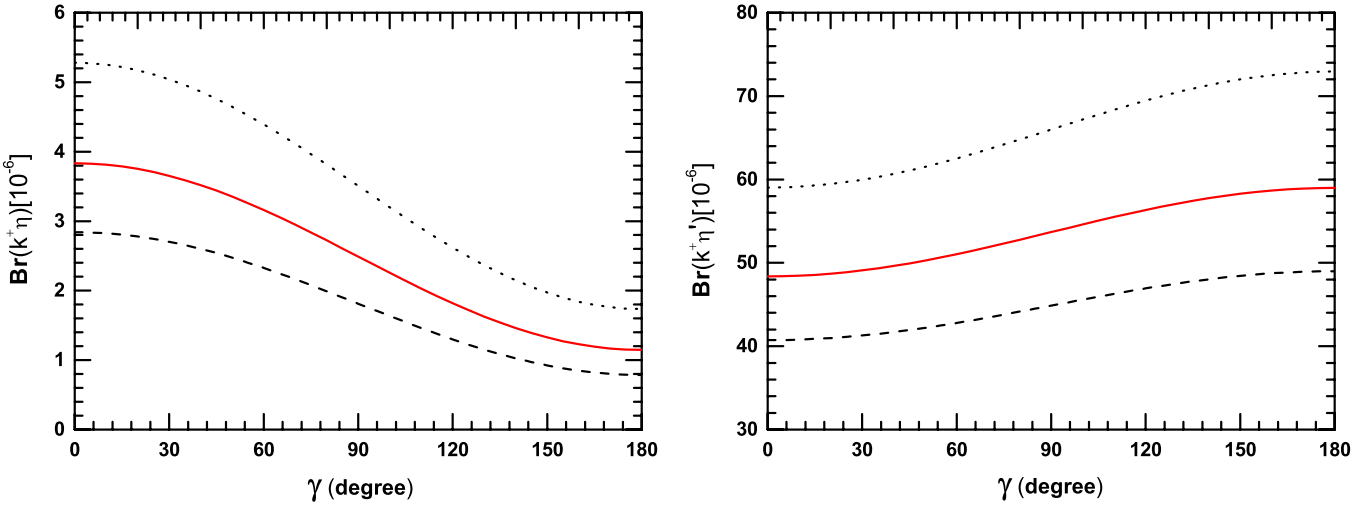

FIG. 9 (color online). The γ dependence of the branching ratios (in units of 10^{-6}) of $B^+ \to K^+\eta^{(\prime)}$ decays for $\omega_b = 0.36$ GeV (dotted curve), 0.40 GeV (solid curve), and 0.44 GeV (dashed curve).

$B \to K\eta'$ ($B \to K\eta$) decays. For $B^0 \to K^0\eta'$ and $B^+ \to K^+\eta'$ decays, the NLO contributions provide a 70% enhancement to their branching ratios . For $B^0 \to K^0\eta$ and $B^+ \to K^+\eta$ decays, on the other hand, the NLO contributions give rise to a 30% reduction to their branching ratios and result in the good agreement between the pQCD predictions and the data.

(iv) The NLO pQCD predictions for branching ratios $\mathrm{Br}(B \to K\eta^{(\prime)})$ agree very well with the measured values within 1 standard deviation. The NLO contributions play an important role in understanding the observed pattern of branching ratios of the four $B \to K\eta^{(\prime)}$ decays.

C. *CP*-violating asymmetries

Now we turn to the evaluations of the *CP*-violating asymmetries of $B \to K\eta^{(\prime)}$ decays in the pQCD approach. For $B^+ \to K^+\eta^{(\prime)}$ decays, the direct *CP*-violating asymmetries $\mathcal{A}_{CP}$ can be defined as

$$\mathcal{A}_{CP}^{\mathrm{dir}} = \frac{|\bar{\mathcal{M}}_f|^2 - |\mathcal{M}_f|^2}{|\bar{\mathcal{M}}_f|^2 + |\mathcal{M}_f|^2}. \tag{81}$$

Using Eq. (81), it is easy to calculate the direct *CP*-violating asymmetries for the considered decays, which are listed in Table II. As a comparison, we also list currently available data [2] and the corresponding QCDF predictions [15].

The NLO pQCD predictions for $\mathcal{A}_{CP}^{\mathrm{dir}}(B^+ \to K^+\eta^{(\prime)})$ (in units of 10^{-2}) with the major theoretical errors are

$$\begin{aligned}\mathcal{A}_{CP}^{\mathrm{dir}}(B^\pm \to K^\pm\eta) &= -11.7^{+6.8}_{-9.6}(m_s)^{+3.9}_{-4.2}(\gamma)^{+2.9}_{-5.6}(a_2^{\eta_q}),\\ \mathcal{A}_{CP}^{\mathrm{dir}}(B^\pm \to K^\pm\eta') &= -6.2^{+1.2}_{-1.1}(m_s)^{+1.3}_{-1.0}(\gamma)^{+1.3}_{-1.0}(a_2^{\eta_q}),\end{aligned} \tag{82}$$

where the dominant errors come from the variations of $m_s = 130 \pm 30$ MeV, $\gamma = 60° \pm 20°$ and Gegenbauer coefficient $a_2^{\eta_q} = 0.44 \pm 0.22$, respectively.

As to the *CP*-violating asymmetries for the neutral decays $B^0 \to K^0\eta^{(\prime)}$, the effects of $B^0 - \bar{B}^0$ mixing should be considered. The *CP*-violating asymmetry of $B^0(\bar{B}^0) \to K^0\eta^{(\prime)}$ decays are time-dependent and can be defined as

$$\begin{aligned}A_{CP} &\equiv \frac{\Gamma(\bar{B}_d^0(\Delta t) \to f_{CP}) - \Gamma(B_d^0(\Delta t) \to f_{CP})}{\Gamma(\bar{B}_d^0(\Delta t) \to f_{CP}) + \Gamma(B_d^0(\Delta t) \to f_{CP})}\\ &= A_{CP}^{\mathrm{dir}}\cos(\Delta m \Delta t) + A_{CP}^{\mathrm{mix}}\sin(\Delta m \Delta t),\end{aligned} \tag{83}$$

where Δm is the mass difference between the two B_d^0 mass eigenstates, $\Delta t = t_{CP} - t_{\mathrm{tag}}$ is the time difference between the tagged B^0 ($\bar{B}^0$) and the accompanying $\bar{B}^0$ (B^0) with opposite b flavor decaying to the final *CP*-eigenstate f_{CP} at the time t_{CP}. The direct and mixing-induced *CP*-violating asymmetries $\mathcal{A}_{CP}^{\mathrm{dir}}$ (or $\mathcal{A}_f$ in terms of Belle Collaboration) and $\mathcal{A}_{CP}^{\mathrm{mix}}$ can be written as

TABLE II. The pQCD predictions for the direct *CP* asymmetries in the NDR scheme (in units of 10^{-2}), the QCDF predictions [15], and the world average as given by HFAG [2].

Mode	LO	$\mathrm{LO}_{\mathrm{NLOWC}}$	+VC	+QL	+MP	NLO	Data	QCDF
$\mathcal{A}_{CP}^{\mathrm{dir}}(B^\pm \to K^\pm\eta)$	9.3	10.3	31.1	7.8	7.6	-11.7	-27 ± 9	$-18.9^{+29.0}_{-30.0}$
$\mathcal{A}_{CP}^{\mathrm{dir}}(B^\pm \to K^\pm\eta')$	-10.1	-7.3	-10.6	-5.9	-10.4	-6.2	1.6 ± 1.9	$-9.0^{+10.6}_{-16.2}$

TABLE III. The pQCD predictions for the direct, mixing-induced and total *CP* asymmetries (in units of 10^{-2}) for $B^0 \to K^0\eta^{(\prime)}$ decays, and the world average as given by HFAG [2].

Mode	LO	LO_{NLOWC}	+VC	+QL	+MP	NLO	Data
$\mathcal{A}_{CP}^{\text{dir}}(B^0 \to K_S^0\eta)$	-4.2	-1.5	-11.2	-0.9	-1.9	-12.7	$\cdots$
$\mathcal{A}_{CP}^{\text{dir}}(B^0 \to K_S^0\eta')$	1.4	0.0	1.5	0.7	-0.1	2.3	9 ± 6
$\mathcal{A}_{CP}^{\text{mix}}(B^0 \to K_S^0\eta)$	61.6	67.3	64.4	66.9	67.9	61.9	$\cdots$
$\mathcal{A}_{CP}^{\text{mix}}(B^0 \to K_S^0\eta')$	64.6	63.5	63.4	63.2	63.2	62.7	61 ± 7
$\mathcal{A}_{CP}^{\text{tot}}(B^0 \to K_S^0\eta)$	27.2	31.7	24.2	31.9	31.7	22.1	$\cdots$
$\mathcal{A}_{CP}^{\text{tot}}(B^0 \to K_S^0\eta')$	32.1	30.8	31.7	31.0	30.5	31.8	$\cdots$

$$\mathcal{A}_{CP}^{\text{dir}} = \mathcal{A}_f = \frac{|\lambda_{CP}|^2 - 1}{1 + |\lambda_{CP}|^2},$$
$$\mathcal{A}_{CP}^{\text{mix}} = \mathcal{S}_f = \frac{2\,\text{Im}(\lambda_{CP})}{1 + |\lambda_{CP}|^2}, \tag{84}$$

with the *CP*-violating parameter λ_{CP}

$$\lambda_{CP} \equiv \left(\frac{q}{p}\right)_d \cdot \frac{\langle f_{CP}|H_{\text{eff}}|\bar{B}^0\rangle}{\langle f_{CP}|H_{\text{eff}}|B^0\rangle}. \tag{85}$$

By integrating the time variable t, one finds the total *CP* asymmetries for $B^0 \to K^0\eta^{(\prime)}$ decays,

$$\mathcal{A}_{CP}^{\text{tot}} = \frac{1}{1+x^2}A_{CP}^{\text{dir}} + \frac{x}{1+x^2}A_{CP}^{\text{mix}}, \tag{86}$$

where $x = \Delta m/\Gamma = 0.775$ [40].

In Table III, we show the pQCD predictions for the central values of the direct, mixing-induced, and total *CP* asymmetries for $B^0 \to K_S^0\eta^{(\prime)}$ decays, obtained by using the LO or NLO Wilson coefficients, and adding the vertex corrections, the quark-loops, the magnetic penguin, or include all the mentioned NLO corrections, respectively.

The NLO pQCD predictions for $\mathcal{A}_{CP}^{\text{dir}}(B^0 \to K^0\eta^{(\prime)})$ and $\mathcal{A}_{CP}^{\text{mix}}(B^0 \to K^0\eta^{(\prime)})$ (in units of 10^{-2}) with the major theoretical errors are

$$\mathcal{A}_{CP}^{\text{dir}}(B^0 \to K_S^0\eta) = -12.7 \pm 4.1(m_s)^{+3.2}_{-1.5}(\gamma)^{+3.2}_{-6.7}(a_2^{\eta_q}),$$
$$\mathcal{A}_{CP}^{\text{dir}}(B^0 \to K_S^0\eta') = 2.3^{+0.5}_{-0.4}(m_s)^{+0.3}_{-0.6}(\gamma)^{+0.2}_{-0.1}(a_2^{\eta_q}),$$
$$\mathcal{A}_{CP}^{\text{mix}}(B^0 \to K_S^0\eta) = 61.9^{+35.8}_{-65.0}(\gamma)^{+35.3}_{-64.3}(\alpha),$$
$$\mathcal{A}_{CP}^{\text{mix}}(B^0 \to K_S^0\eta') = 62.7^{+35.5}_{-65.0}(\gamma)^{+35.4}_{-64.7}(\alpha), \tag{87}$$

where the dominant errors come from the variations of $m_s = 130 \pm 30$ MeV, $\gamma = 60° \pm 20°$, $\alpha = 100° \pm 20°$, and the Gegenbauer coefficient $a_2^{\eta_q} = 0.44 \pm 0.22$, respectively.

In Fig. 10, we show the γ-dependence of the pQCD predictions for direct *CP*-violating asymmetries of $B^0 \to K_S^0\eta^{(\prime)}$ and $B^+ \to K^+\eta^{(\prime)}$ decays. In Fig. 11, we show the α-dependence of the total *CP*-violating asymmetries for $B^0 \to K_S^0\eta$ (solid curve) and $B^0 \to K_S^0\eta'$ (dotted curve), respectively.

From the pQCD predictions and currently available experimental measurements for the *CP*-violating asymmetries of the four $B \to K\eta^{(\prime)}$ decays, one can see the following points:

(a) For $B^+ \to K^+\eta$ decay, the measured direct *CP* asymmetry is 3 standard deviations from zero. The LO pQCD prediction changed its sign and becomes consistent with the measured one due to the inclusion of NLO contributions.

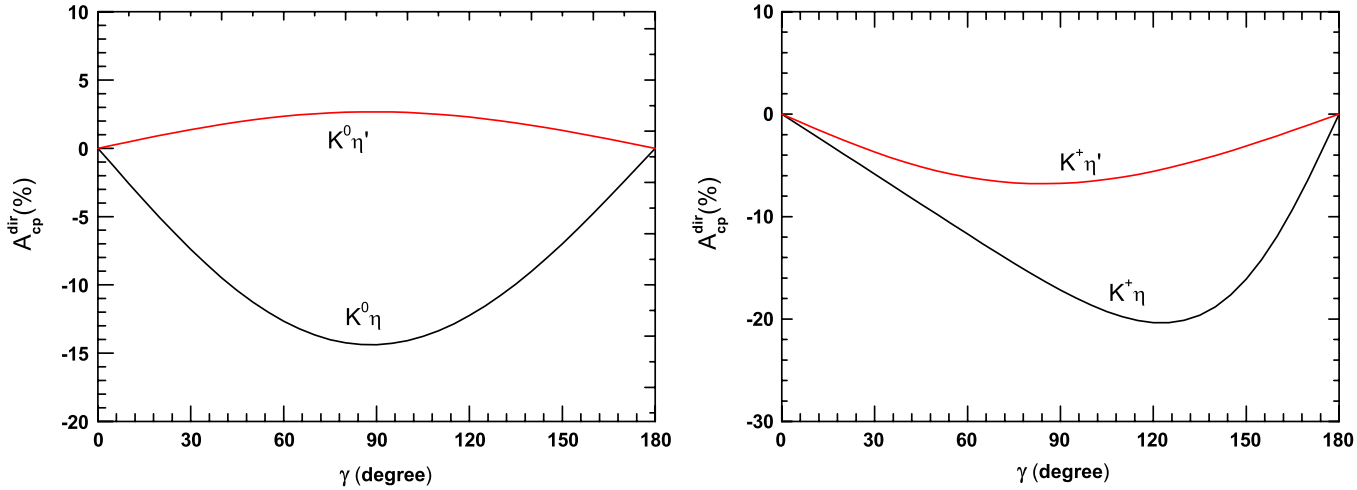

FIG. 10 (color online). The NLO pQCD predictions for direct *CP* asymmetries (in percentage) of $B^0 \to K_S^0\eta^{(\prime)}$ and $B^\pm \to K^\pm\eta^{(\prime)}$ decays.

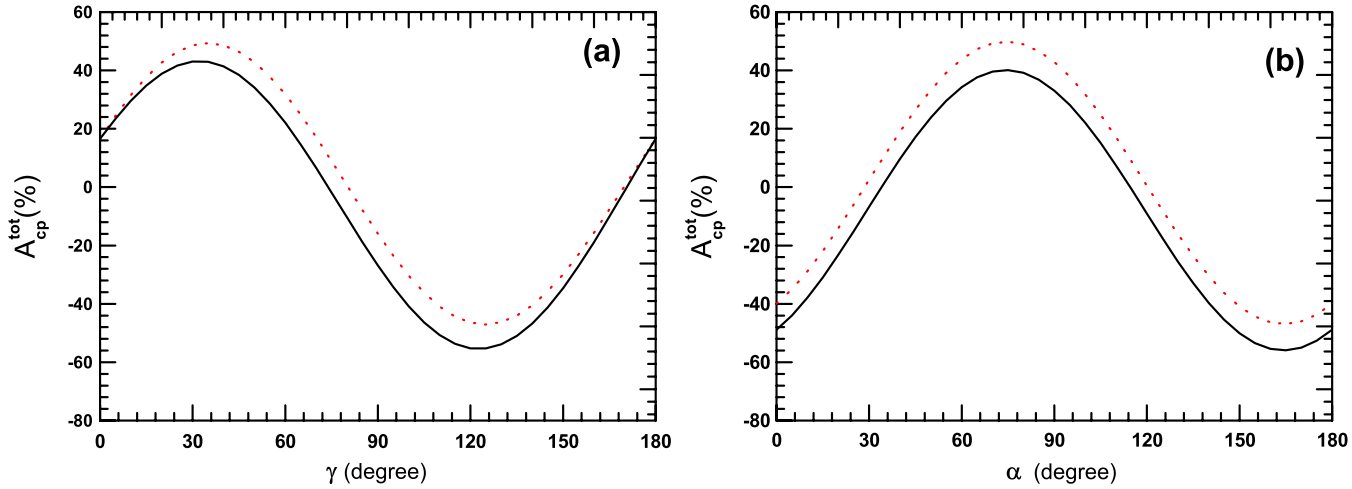

FIG. 11 (color online). The γ-dependence (a) and the α-dependence (b) of the total CP-asymmetries of $B^0 \to K_S^0\eta$ (solid curve) and $B^0 \to K_S^0\eta'$ (dotted curve) decays.

(b) For $\mathcal{A}_{CP}^{\rm dir}(B^\pm \to K^\pm\eta')$, the pQCD prediction is changed from -10% to -6% due to the inclusion of NLO contributions, which is consistent with the measured zero result within 1 standard deviation.

(c) For $B^0 \to K^0\eta^{(\prime)}$ decay, the effects of NLO contributions to their CP asymmetries are rather small, as can be seen from the numerical results as given in Table III.

(d) For neutral $B^0 \to K^0\eta^{(\prime)}$ decays, the PQCD predictions are $\mathcal{A}_{CP}^{\rm dir}(B^0 \to K_S^0\eta') \approx 2.3\%$ and $\mathcal{A}_{CP}^{\rm mix}(B^0 \to K_S^0\eta') \approx 63\%$, which agree very well with the data: $(9 \pm 6)\%$ and $(61 \pm 7)\%$. This means that the deviation $\Delta S = -\eta_f S_f - \sin 2\beta$ for $B^0 \to K^0\eta'$ decay is also very small in the pQCD approach.

VI. SUMMARY

In this paper, we calculated the branching ratios and CP-violating asymmetries of $B^+ \to K^+\eta^{(\prime)}$ and $B^0 \to K^0\eta^{(\prime)}$ decays in the pQCD approach. The partial NLO contributions considered here include QCD vertex corrections, the quark-loops, and the chromomagnetic penguins.

From our calculations and phenomenological analysis, we found the following results:

(a) For branching ratios, the NLO pQCD predictions (in units of 10^{-6}) are

$$\begin{aligned} {\rm Br}(B^+ \to K^+\eta) &= 3.2^{+3.2}_{-1.8}, \\ {\rm Br}(B^\pm \to K^\pm\eta') &= 51.0^{+18.0}_{-10.9}, \\ {\rm Br}(B^0 \to K^0\eta) &= 2.1^{+2.6}_{-1.5}, \\ {\rm Br}(B^0 \to K^0\eta') &= 50.3^{+16.8}_{-10.6}, \end{aligned} \tag{88}$$

where the individual theoretical errors have been added in quadrature. The decay amplitude $B \to K\eta_q$ and $B \to K\eta_s$ interfere constructively for $B \to K\eta'$ decays, but destructively for $B \to K\eta$ decays. The NLO contributions in the pQCD approach, furthermore, can provide a 70% enhancement to ${\rm Br}(B \to K\eta')$, but a 30% reduction to ${\rm Br}(B \to K\eta)$. The large branching ratio of $B \to K\eta'$ decays, as well as the large disparity ${\rm Br}(B \to K\eta') \gg {\rm Br}(B \to K\eta)$ can therefore be understood naturally.

(b) The pQCD predictions for the CP asymmetries of $B \to K\eta^{(\prime)}$ decays are consistent with currently available data. For neutral $B^0 \to K^0\eta^{(\prime)}$ decays, for example, the PQCD predictions are $\mathcal{A}_{CP}^{\rm dir}(B^0 \to K_S^0\eta') \approx 2.3\%$ and $\mathcal{A}_{CP}^{\rm mix}(B^0 \to K_S^0\eta') \approx 63\%$, which agree very well with the measured values of $(9 \pm 6)\%$ and $(61 \pm 7)\%$, respectively.

(c) In this paper, only the partial NLO contributions in the pQCD approach have been taken into account. These considered NLO contributions may be the dominant part of the whole NLO corrections. To achieve a complete NLO calculation in the pQCD approach, of course, the still-missing pieces from the emission diagrams, hard-spectator and annihilation diagrams, should be evaluated as soon as possible.

ACKNOWLEDGMENTS

The authors are very grateful to Hsiang-nan Li, Cai-Dian Lü, Ying Li, Wei Wang and Yu-Ming Wang for helpful discussions. This work is partly supported by the National Natural Science Foundation of China under Grant No. 10575052 and 10735080.

APPENDIX: RELATED FUNCTIONS

We show here the function h_is, coming from the Fourier transformations of the hard kernel $H^{(0)}(x_i, b_i)$,

$$h_e(x_1, x_2, b_1, b_2) = K_0(\sqrt{x_1 x_2} m_B b_1)[\theta(b_1 - b_2) K_0(\sqrt{x_2} m_B b_1) I_0(\sqrt{x_2} m_B b_2) + \theta(b_2 - b_1) K_0(\sqrt{x_2} m_B b_2) I_0(\sqrt{x_2} m_B b_1)] S_t(x_2), \tag{A1}$$

$$h_a(x_2, x_3, b_2, b_3) = K_0(i\sqrt{(1 - x_2)x_3} m_B b_2)[\theta(b_3 - b_2) K_0(i\sqrt{x_3} m_B b_3) I_0(i\sqrt{x_3} m_B b_2) + \theta(b_2 - b_3) K_0(i\sqrt{x_3} m_B b_2) I_0(i\sqrt{x_3} m_B b_3)] S_t(x_3), \tag{A2}$$

$$h_f(x_1, x_2, x_3, b_1, b_3) = \{\theta(b_1 - b_3) K_0(M_B\sqrt{x_1 x_2} b_1) I_0(M_B\sqrt{x_1 x_2} b_3) + \theta(b_3 - b_1) K_0(M_B\sqrt{x_1 x_2} b_3) I_0(M_B\sqrt{x_1 x_2} b_1)\} \cdot \begin{pmatrix} \frac{\pi i}{2} H_0(\sqrt{(x_2(x_3 - x_1))} M_B b_3), & \text{for } x_1 - x_3 < 0 \\ K_0^{(1)}(\sqrt{(x_2(x_1 - x_3)} M_B b_3), & \text{for } x_1 - x_3 > 0 \end{pmatrix}, \tag{A3}$$

$$h_f^3(x_1, x_2, x_3, b_1, b_3) = \{\theta(b_1 - b_3) K_0(i\sqrt{(1 - x_2)x_3} b_1 M_B) I_0(i\sqrt{(1 - x_2)x_3} b_3 M_B) + (\theta(b_3 - b_1) K_0(i\sqrt{(1 - x_2)x_3} b_3 M_B) I_0(i\sqrt{(1 - x_2)x_3} b_1 M_B)\} \cdot \begin{pmatrix} K_0(M_B\sqrt{(x_1 - x_3)(1 - x_2)} b_1), & \text{for } x_1 - x_3 > 0 \\ \frac{\pi i}{2} H_0^{(1)}(M_B\sqrt{(x_3 - x_1)(1 - x_2)} b_1), & \text{for } x_1 - x_3 < 0 \end{pmatrix}, \tag{A4}$$

$$h_f^4(x_1, x_2, x_3, b_1, b_2) = \{\theta(b_1 - b_3) K_0(i\sqrt{(1 - x_2)x_3} b_1 M_B) I_0(i\sqrt{(1 - x_2)x_3} b_3 M_B) + \theta(b_3 - b_1) K_0(i\sqrt{(1 - x_2)x_3} b_3 M_B) I_0(i\sqrt{(1 - x_2)x_3} b_1 M_B)\} \cdot \begin{pmatrix} K_0(M_B F_1 b_1), & \text{for } F_1^2 > 0 \\ \frac{\pi i}{2} H_0^{(1)}(M_B\sqrt{|F_1^2|} b_1), & \text{for } F_1^2 < 0 \end{pmatrix}, \tag{A5}$$

where J_0 is the Bessel function and K_0, I_0 are modified Bessel functions with $K_0(-ix) = -(\pi/2)Y_0(x) + i(\pi/2)J_0(x)$, and $F_{(1)}$'s are defined by

$$F_{(1)}^2 = 1 - x_2(1 - x_1 - x_3). \tag{A6}$$

The threshold resummation form factor $S_t(x_i)$ is adopted from Ref. [41]. It has been parametrized as

$$S_t(x) = \frac{2^{1+2c}\Gamma(3/2 + c)}{\sqrt{\pi}\Gamma(1 + c)}[x(1 - x)]^c, \tag{A7}$$

where the parameter $c = 0.3$. This function is normalized to unity.

The evolution factors $E_e^{(\prime)}$, and $E_a^{(\prime)}$, appeared in the decay amplitudes are given by

$$\begin{aligned} E_e(t) &= \alpha_s(t) \exp[-S_{ab}(t)], \\ E_e'(t) &= \alpha_s(t) \exp[-S_{cd}(t)]|_{b_2 = b_1}, \\ E_a'(t) &= \alpha_s(t) \exp[-S_{ef}(t)]|_{b_2 = b_3}, \\ E_a(t) &= \alpha_s(t) \exp[-S_{gh}(t)]. \end{aligned} \tag{A8}$$

The Sudakov factors used in the text are defined as

$$S_{ab}(t) = s(x_1 m_B/\sqrt{2}, b_1) + s(x_2 m_B/\sqrt{2}, b_2) + s((1 - x_2) m_B/\sqrt{2}, b_2) - \frac{1}{\beta_1}\left[\ln\frac{\ln(t/\Lambda)}{-\ln(b_1\Lambda)} + \ln\frac{\ln(t/\Lambda)}{-\ln(b_2\Lambda)}\right], \tag{A9}$$

$$S_{cd}(t) = s(x_1 m_B/\sqrt{2}, b_1) + s(x_2 m_B/\sqrt{2}, b_1) + s((1 - x_2) m_B/\sqrt{2}, b_1) + s(x_3 m_B/\sqrt{2}, b_3) + s((1 - x_3) m_B/\sqrt{2}, b_3) - \frac{1}{\beta_1}\left[2\ln\frac{\ln(t/\Lambda)}{-\ln(b_1\Lambda)} + \ln\frac{\ln(t/\Lambda)}{-\ln(b_3\Lambda)}\right], \tag{A10}$$

$$S_{ef}(t) = s(x_1 m_B/\sqrt{2}, b_1) + s(x_2 m_B/\sqrt{2}, b_3) + s((1 - x_2) m_B/\sqrt{2}, b_3) + s(x_3 m_B/\sqrt{2}, b_3) + s((1 - x_3) m_B/\sqrt{2}, b_3) - \frac{1}{\beta_1}\left[\ln\frac{\ln(t/\Lambda)}{-\ln(b_1\Lambda)} + 2\ln\frac{\ln(t/\Lambda)}{-\ln(b_2\Lambda)}\right], \tag{A11}$$

$$S_{gh}(t) = s(x_2 m_B/\sqrt{2}, b_2) + s(x_3 m_B/\sqrt{2}, b_3) + s((1-x_2)m_B/\sqrt{2}, b_2) + s((1-x_3)m_B/\sqrt{2}, b_3) - \frac{1}{\beta_1}\left[\ln\frac{\ln(t/\Lambda)}{-\ln(b_3\Lambda)} + \ln\frac{\ln(t/\Lambda)}{-\ln(b_2\Lambda)}\right], \tag{A12}$$

where the function $s(q, b)$ is defined in Appendix A of Ref. [29]. The scale t_is in the above equations are chosen as

$$\begin{aligned}
t_a &= \max(\sqrt{x_2}m_B, \sqrt{x_1 x_2}m_B, 1/b_1, 1/b_2),\\
t'_a &= \max(\sqrt{x_1}m_B, \sqrt{x_1 x_2}m_B, 1/b_1, 1/b_2),\\
t_b &= \max(\sqrt{x_2|1-x_3-x_1|}m_B, \sqrt{x_1 x_2}m_B, 1/b_1, 1/b_3),\\
t'_b &= \max(\sqrt{x_2|x_3-x_1|}m_B, \sqrt{x_1 x_2}m_B, 1/b_1, 1/b_3),\\
t_c &= \max(\sqrt{(1-x_2)x_3}m_B, \sqrt{|x_1-x_3|(1-x_2)}m_B, 1/b_1, 1/b_3),\\
t'_c &= \max(\sqrt{|1-x_2(1-x_3-x_1)|}m_B, \sqrt{(1-x_2)x_3}m_B, 1/b_1, 1/b_3),\\
t_d &= \max(\sqrt{(1-x_2)x_3}m_B, \sqrt{(1-x_2)}m_B, 1/b_2, 1/b_3),\\
t'_d &= \max(\sqrt{(1-x_2)x_3}m_B, \sqrt{x_3}m_B, 1/b_2, 1/b_3).
\end{aligned} \tag{A13}$$

[1] B. H. Behrens (CLEO Collaboration), Phys. Rev. Lett. **80**, 3710 (1998).
[2] E. Barberio *et al.*, (Heavy Flavor Averaging Group), arXiv:0704.3575; online update at http://www.slac.stanford.edu/xorg/hfag.
[3] P. Chang *et al.* (Belle Collaboration), Phys. Rev. D **71**, 091106(R) (2005); K.-F. Chen *et al.* (Belle Collaboration), Phys. Rev. Lett. **98**, 031802 (2007); B. Aubert *et al.* (*BABAR* Collaboration), Phys. Rev. D **76**, 031103(R) (2007); Phys. Rev. Lett. **98**, 031801 (2007).
[4] H. J. Lipkin, Phys. Lett. B **254**, 247 (1991).
[5] Y. Grossman and M. P. Worah, Phys. Lett. B **395**, 241 (1997).
[6] D. Atwood and A. Soni, Phys. Lett. B **405**, 150 (1997); W. S. Hou and B. Tseng, Phys. Rev. Lett. **80**, 434 (1998).
[7] F. Yuan and K. T. Chao, Phys. Rev. D **56**, R2495 (1997); I. Halperin and A. Zhitnitsky, Phys. Rev. D **56**, 7247 (1997); Phys. Rev. Lett. **80**, 438 (1998).
[8] A. Ali, J. Chay, C. Greub, and P. Ko, Phys. Lett. B **424**, 161 (1998).
[9] D. S. Du, C. S. Kim, and Y. D. Yang, Phys. Lett. B **426**, 133 (1998).
[10] M. Z. Yang and Y. D. Yang, Nucl. Phys. **B609**, 469 (2001).
[11] M. R. Ahmady, E. Kou, and A. Sugamoto, Phys. Rev. D **58**, 014015 (1998).
[12] A. L. Kagan and A. A. Petrov, arXiv:hep-ph/9707354; S. Khalil and E. Kou, Phys. Rev. Lett. **91**, 241602 (2003).
[13] G. R. Lu, Z. J. Xiao, H. K. Guo, and L. X. Lü, J. Phys. G **25**, L85 (1999); Z. J. Xiao, K. T. Chao, and C. S. Li, Phys. Rev. D **65**, 114021 (2002); Z. J. Xiao and W. J. Zou, Phys. Rev. D **70**, 094008 (2004).
[14] M. Beneke and M. Neubert, Nucl. Phys. **B651**, 225 (2003).
[15] M. Beneke and M. Neubert, Nucl. Phys. **B675**, 333 (2003).
[16] E. Kou and A. Sanda, Phys. Lett. B **525**, 240 (2002).
[17] M. Beneke, G. Buchalla, M. Neubert, and C. T. Sachrajda, Phys. Rev. Lett. **83**, 1914 (1999).
[18] H. N. Li, Prog. Part. Nucl. Phys. **51**, 85 (2003) and references therein.
[19] T. Feldmann, P. Kroll, and B. Stech, Phys. Rev. D **58**, 114006 (1998); T. Feldmann, Int. J. Mod. Phys. A **15**, 159 (2000).
[20] R. Escribano and J. M. Frere, J. High Energy Phys. 06 (2005) 029; J. Schechter, A. Subbaraman, and H. Weigel, Phys. Rev. D **48**, 339 (1993).
[21] Y. Y. Charng, T. Kurimoto, and H. N. Li, Phys. Rev. D **74**, 074024 (2006); **78**, 059901(E) (2008).
[22] P. Ball and G. W. Jones, J. High Energy Phys. 08 (2007) 025.
[23] A. G. Akeroyd, C. H. Chen, and C. Q. Geng, Phys. Rev. D **75**, 054003 (2007).
[24] J. F. Hsu, Y. Y. Charng, and H. N. Li, Phys. Rev. D **78**, 014020 (2008).
[25] H. N. Li, S. Mishima, and A. I. Sanda, Phys. Rev. D **72**, 114005 (2005).
[26] M. Beneke, Phys. Lett. B **620**, 143 (2005); G. Buchalla *et al.*, J. High Energy Phys. 09 (2005) 074; H. Y. Cheng, C. K. Chua, and A. Soni, Phys. Rev. D **72**, 014006 (2005).
[27] A. R. Williamson and J. Zupan, Phys. Rev. D **74**, 014003 (2006).
[28] Y.-Y. Keum, H. N. Li, and A. I. Sanda, Phys. Rev. D **63**, 054008 (2001).
[29] C. D. Lü, K. Ukai, and M. Z. Yang, Phys. Rev. D **63**, 074009 (2001).
[30] X. Liu, H. S. Wang, Z. J. Xiao, L. B. Guo, and C. D. Lü,

Phys. Rev. D **73**, 074002 (2006); H. S. Wang, X. Liu, Z. J. Xiao, L. B. Guo, and C. D. Lü, Nucl. Phys. **B738**, 243 (2006).
[31] Z. J. Xiao, D. Q. Guo, and X. F. Chen, Phys. Rev. D **75**, 014018 (2007); D. Q. Guo, X. F. Chen, and Z. J. Xiao, Phys. Rev. D **75**, 054033 (2007); X. F. Chen, D. Q. Guo, and Z. J. Xiao, Eur. Phys. J. C **50**, 363 (2007).
[32] G. Buchalla, A. J. Buras, and M. E. Lautenbacher, Rev. Mod. Phys. **68**, 1125 (1996).
[33] M. Beneke, Nucl. Phys. B, Proc. Suppl. **170**, 57 (2007).
[34] Z. Q. Zhang and Z. J. Xiao, arXiv:0807.2022.
[35] Z. Q. Zhang and Z. J. Xiao, arXiv:0807.2024.
[36] C. D. Lü and M. Z. Yang, Eur. Phys. J. C **28**, 515 (2003).
[37] P. Ball, V. M. Braun, Y. Koike, and K. Tanaka, Nucl. Phys. **B529**, 323 (1998); P. Ball, J. High Energy Phys. 09 (1998) 005; 01 (1999) 010; P. Ball and R. Zwicky, Phys. Rev. D **71**, 014015 (2005); J. High Energy Phys. 04 (2006) 046.
[38] S. Mishima and A. I. Sanda, Prog. Theor. Phys. **110**, 549 (2003).
[39] M. Bander, D. Silverman, and A. Soni, Phys. Rev. Lett. **43**, 242 (1979); J. M. Gerard and W. S. Hou, Phys. Rev. D **43**, 2909 (1991).
[40] W.-M. Yao *et al.* (Particle Data Group), J. Phys. G **33**, 1 (2006).
[41] T. Kurimoto, H. N. Li, and A. I. Sanda, Phys. Rev. D **65**, 014007 (2001).